

# **PERFORMANCE OF EARTH MASONRY UNDER DYNAMIC LOADING**

Karapitiye Pathiranage Indunil Erandi Ariyaratne

(178026M)

Degree of Master of Science

Department of Civil Engineering

University of Moratuwa

Sri Lanka

September 2018

**PERFORMANCE OF EARTH MASONRY UNDER  
DYNAMIC LOADING**

Karapitiye Pathirana Indunil Erandi Ariyaratne

(178026M)

Thesis submitted in partial fulfillment of the requirements for the degree Master of  
Science in Civil Engineering

Department of Civil Engineering

University of Moratuwa

Sri Lanka

September 2018

## DECLARATION

I declare that this is my own work and this thesis does not incorporate without acknowledgement any material previously submitted for a Degree or Diploma in any other university or institute of higher learning and to the best of my knowledge and belief it does not contain any material previously published or written by another person except where the acknowledgement is made in the text.

Also, I hereby grant to University of Moratuwa the non-exclusive right to reproduce and distribute the thesis, in whole or in part in print, electronic or other medium. I retain the right to use this content in whole or part in future works (such as articles or books).

Signature:

Date:

The above candidate has carried out research for the Masters under my supervision

Name of the supervisor: Prof. (Mrs.) C. Jayasinghe

Signature of the supervisor:

Date:

Name of the supervisor: Prof. M.T.R. Jayasinghe

Signature of the supervisor:

Date:

Name of the supervisor: Prof. Peter Walker

Signature of the supervisor:

Date:

## **ACKNOWLEDGEMENTS**

Under the Research Project, I had the opportunity of gaining a very valuable experience of how to apply the theoretical knowledge gathered throughout the four years as an undergraduate to produce important findings for the well-being and development of the community.

There are number of persons whom I must pay my gratitude for their help towards the successful completion of the research project and report.

First, I am very grateful for the valuable guidance and encouragement given by my research supervisors, Prof. (Mrs.) C. Jayasinghe, Senior Professor in the Department of Civil Engineering, University of Moratuwa, Prof. M. T. R. Jayasinghe, Senior Professor in the Department of Civil Engineering, University of Moratuwa and Prof. P. Walker, Professor in the Department of Architecture and Civil Engineering, University of Bath. Further I am thankful to senior professor, Prof. A.A.D.J. Perera and senior lecturer, Dr. H.M.Y.C. Mallikarachchi for evaluating and giving us valuable instructions regarding the research findings we presented during the research progress presentations.

Finally, I pay my appreciation to Mr.T.P.D.G. Indika Yohan, M.L. Perera, P.P.R. Peris and D.U. Jayasinghe, non-academic staff of Department of Civil Engineering, University of Moratuwa who helped us in experimental work.

Ariyaratne, K.P.I.E.  
Department of Civil Engineering  
University of Moratuwa  
06.09.2018



## ABSTRACT

Masonry buildings are the most typical structural type which is commonly used for ancient historical structures and low to medium rise residential units from early days to present. However, increase in world population and their housing needs with limited resources tend to promote the usage of alternative building materials in the construction industry as much as possible. Among those alternatives, earth masonry has become one of the building materials in sustainable development process since its in-built properties such as economy, low embodied energy, low in CO<sub>2</sub> emissions, etc. However, the structural elements made from earth masonry such as rammed earth and compressed earth blocks (stabilized/un-stabilized), have not been much assessed on their seismic performance.

The main objective is to comparatively assess the in-plane and out-of-plane seismic performance of Cement Stabilized Earth Blocks (CSEB) and Cement Stabilized Rammed Earth (CSRE) walls with similar dimension via a series of shake table test and to recommend a most suitable numerical method for analysing the seismic performance of CSEB and CSRE walls.

For this purpose, a set of small scale physical models of compressed stabilized earth blocks and rammed earth were tested under scaled versions of El-Centro (EIC) earthquake north-south component and sine waves with different frequencies and amplitudes using one degree of freedom shaking table equipment.

For experiments, 110 mm thick compressed stabilized earth blocks and 150 mm thick rammed earth wall panels were selected. Two wall panels of each earth masonry type were prepared for around 596mm and 460mm height respectively. A 38 mm thick concrete layer was laid bottom and top of each specimen for confinement of the element. The tests were carried out under series of shake table tests and observed the deflection and acceleration behaviour at bottom, middle and top of wall panels, base shear values, failure mode and magnitude.

According to the experimental results from moderate to severe earthquakes, both CSEB and CSRE wall panels performed well without any visible cracks. In CSEB wall panels, maximum acceleration and displacement at the crest of the wall and base shear is 8.2%, 1.2% and 7.6% greater in out-of-plane loads than the in-plane walls under severe earthquake. But in RE wall panels those above considered values remain same for both in and out-of-plane walls.

To investigate the progressive damage behavior of earth walls, they subjected to sine waves with increasing amplitudes and frequencies. In CSEB walls, there were no visible cracks both in and out-of-plane walls until the 4Hz sine wave. But when the frequency become 6Hz, base crack was initiated and spread throughout the wall width in the out-of-plane wall and no visible cracks in the in - plane wall. In RE walls, there were no visible cracks both in and out-of-plane walls until the 4Hz sine wave. But when the frequency become 6Hz, base crack was developed through the wall width with rocking mode in the out-of-plane wall and base crack was developed with some translation to the loading direction in the in-plane wall.

Numerical models were prepared with Structural Analysis Program (SAP 2000) and ABAQUS with the intension of using experimental results to validate. It is found the ABAQUS model is capable of predicting the behaviour of earth masonry under seismic loading.

**Key words:** Earth masonry, Shake table test, In-plane loading, Out-of-plane loading, Numerical modelling.

## TABLE OF CONTENTS

DECLARATION .....	i
ACKNOWLEDGEMENTS .....	ii
ABSTRACT .....	iii
TABLE OF CONTENTS.....	iv
LIST OF FIGURES.....	vi
LIST OF TABLES.....	vii
LIST OF ABBREVIATIONS.....	vii
LIST OF APPENDICES.....	vii
1. INTRODUCTION.....	1
1.1 RESEARCH BACKGROUND .....	1
1.2 OBJECTIVE.....	2
1.3 METHODOLOGY .....	2
1.4 THE ARRANGEMENT OF THE THESIS .....	3
2. LITERATURE REVIEW .....	4
2.1 INTRODUCTION.....	4
2.2 SEISMIC PERFORMANCE OF MASONRY STRUCTURES .....	5
2.2.1 CONVENTIONAL MATERIALS .....	5
2.2.2 EARTH MATERIALS .....	14
2.2.3 OBSERVED TRENDS IN DYNAMIC PERFORMANCE OF MASONRY STRUCTURES THROUGH EXPERIMENTAL STUDIES.....	21
2.2.4 SUMMARY OF IDEALIZATIONS USED IN NUMERICAL MODELLING OF MASONRY STRUCTURES.....	22
3. EXPERIMENTAL STUDY .....	25
3.1 INTRODUCTION.....	25
3.2 SELECTION OF PARAMETERS .....	25
3.2.1 COMPRESSED STABILIZED EARTH BLOCKS WALL PANELS.....	25
3.2.2 RAMMED EARTH WALL PANELS .....	26
3.3 MATERIAL PROPERTIES .....	27
3.3.1 CSEB .....	27
3.3.2 CSRE.....	28
3.4 TEST SET UP.....	30
3.5 CONSTRUCTION SEQUENCE.....	36
3.5.1 CSEB WALLS .....	36
3.5.2 CSRE WALLS .....	38
3.6 SEQUENCE OF LOADING .....	40
3.7 SUMMARY .....	42
4. RESULTS AND DISCUSSION.....	43
4.1 GENERAL.....	43
4.2 PERFORMANCE OF CSEB WALLS UNDER SEISMIC LOADS.....	43
4.3 PERFORMANCE OF STABILIZED RAMMED EARTH WALLS UNDER SEISMIC LOADS.....	44

4.4	COMPARISON OF RESULTS .....	45
4.5	SUMMARY .....	48
5.	NUMERICAL MODELLING .....	49
5.1.1	DEFINING NEW MODEL .....	50
5.1.2	GEOMETRY .....	51
5.1.3	MATERIAL PROPERTIES .....	51
5.1.4	RESTRAINTS .....	52
5.1.5	LOADING .....	53
5.2	THE PROCESS OF NUMERICAL MODELLING IN ABAQUS .....	56
5.2.1	STRUCTURAL ANALYSIS USING ABAQUS .....	56
5.2.2	GEOMETRY .....	57
5.2.3	MATERIAL PROPERTIES .....	57
5.2.4	ASSEMBLING OF THE REAL OBJECT .....	58
5.2.5	INTERACTION .....	59
5.2.6	LOADING .....	59
5.2.7	MESHING .....	60
5.3	COMPARISON OF SAP AND ABAQUS NUMERICAL RESULTS .....	61
6.	CONCLUSION AND FUTURE WORK .....	68
6.1	FUTURE WORK .....	69
	REFERENCE LIST .....	70
	ANNEXURE .....	74
	APPENDIX A: El-Centro earthquake data .....	75
	APPENDIX B: Acceleration and displacement results of CSEB wall panels under moderate sized earthquake .....	77
	APPENDIX C: El-Centro earthquake full data sheet and acceleration and displacement results of CSEB and CSRE wall panels from moderate to severe sized earthquake (CD Attachment)	

## LIST OF FIGURES

Page

Figure 1.1: Damaged structures due to Nepal earthquake in 2015.....	2
Figure 1.2 : Flow Chart of Methodology .....	3
Figure 2.1 : Prevailing Studies relevant to Seismic Performance of Masonry Structures.....	4
Figure 2.2: Experimental set up with steel frames .....	5
Figure 2.3: FEM (ABAQUS with explicit solver with openings).....	7
Figure 2.4: New construction method with trussed reinforcement.....	8
Figure 2.5: Experimental setup and discrete model .....	11
Figure 2.6: Un-bonded brick work and interlocking masonry unit .....	11
Figure 2.7: Non-retrofitted and retrofitted walls and the numerical model.....	13
Figure 2.8: Experimental wall and the numerical model.....	14
Figure 2.9: Experimental and numerical model .....	15
Figure 2.10: Load application using hydraulic jack .....	16
Figure 2.11 : Wall panel sections selected for Research .....	23
Figure 3.1: Geometry of CSEB wall panels .....	26
Figure 3.2: Geometry of CSRE wall panels .....	27
Figure 3.3: Jar Test.....	28
Figure 3.4: Casting of CSRE cubes.....	29
Figure 3.5: Moratuwa University one-degree shaking table .....	30
Figure 3.6: Equalization of Input and Output signals.....	35
Figure 3.7: Construction steps of CSEB wall panel .....	37
Figure 3.8: Construction steps of CSRE wall panels .....	39
Figure 3.9: Final view of wall specimens.....	40
Figure 3.10: Test specimens loading directions .....	42
Figure 4.1: Variation of acceleration and displacement in CSEB panels.....	43
Figure 4.2: Base crack in CSEB out-of-plane wall .....	44
Figure 4.3: Variation of acceleration and displacement in RE panels.....	44
Figure 4.4: Base crack in CSRE wall panels.....	45
Figure 4.5: Base Shear distribution during load category 1 .....	47
Figure 5.1: Steps in SAP model .....	50
Figure 5.2: Grid type model .....	51
Figure 5.3: Block and mortar as one unit .....	51
Figure 5.4 : Defining material properties .....	52
Figure 5.5: Effect of edge area constraint .....	52
Figure 5.6: Steps in defining the loading.....	54
Figure 5.7: Analysis of SAP results .....	55
Figure 5.8: Steps of ABAQUS Modelling .....	56
Figure 5.9: Defining the units .....	57
Figure 5.10: Tensile and compression behaviour in CDP model .....	58
Figure 5.11: Assembly of the real object in ABAQUS .....	58
Figure 5.12: Loading in ABAQUS.....	59
Figure 5.13: Meshing the object in ABAQUS .....	60
Figure 5.14: Analysis of ABAQUS results .....	60
Figure 5.15: SAP numerical results.....	61
Figure 5.16: ABAQUS numerical results.....	62
Figure 5.17: CSEB wall numerical model.....	65
Figure 5.18: CSEB Displacement vs. Time.....	66

Figure 5.19: CSRE Displacement vs. Time.....	66
Figure 5.20: Failure Stresses of CSEB walls.....	67
Figure 5.21: Failure Stresses of CSRE walls.....	67

## LIST OF TABLES

	Page
Table 2.1: Observations of each model .....	12
Table 2.2: Collapse frequencies for single room models with different blocks .....	17
Table 2.3: Summary of few experimental and numerical research studies carried out relevant to the dynamic performance of different masonry structures .....	20
Table 2.4: Experimental results for different elements retrofitted with FRP .....	21
Table 3.1: Loading Steps.....	41
Table 4.1: Responses during loading category 1 .....	46
Table 4.2: Occurrence of visible cracks .....	47
Table 5.1: Comparison of two computational models.....	63
Table 5.2: Comparison of Numerical Modelling Results with Experimental .....	66

## LIST OF ABBREVIATIONS

Abbreviation	Description
CSEB	Cement Stabilized Earth Block
CSRE	Cement Stabilized Rammed Earth
EQRF	Earthquake Resistant Feature
EIC	El-Centro
FEM	Finite Element Method
FRP	Fibre Reinforced Polymer
GFRP	Glass Fibre Reinforced Polymer
PGA	Peak Ground Acceleration
PP	Polypropylene
NZS	New Zealand Standard
RM	Reinforced Masonry
SAP	Structural Analysis Program
SLS	Serviceability Limit State
URM	Unreinforced Masonry

## LIST OF APPENDICES

Appendix	Description	Page
Appendix A	El-Centro earthquake data	75
Appendix B	Acceleration and displacement results of CSEB wall panels under moderate earthquake	77
Appendix C	El-Centro earthquake full data sheet and acceleration and displacement results of CSEB and CSRE wall panels from moderate to severe sized earthquake (CD Attachment)	

# 1. INTRODUCTION

## 1.1 Research Background

Masonry buildings are the most typical structural type which is commonly used in house construction and also found to be the main element for historical structures. The following advantages of masonry may lead to its selection for construction:

- Low cost
- Availability of materials
- Thermal efficiency
- Sound insulation
- Labour intensive construction technology
- Sufficient durability, etc.

However, it is a well-known fact that the construction of masonry buildings tends to consume lots of renewable and non-renewable resources, delivering lots of emissions to the environment creating negative and positive impacts globally. Therefore, Sustainable Building Concepts have been introduced to enhance the positive impacts while mitigating the negative impacts on the earth.

Under this objective designer prefers 'earth masonry' as one of the best building materials in the sustainable development process. Most of the mechanical properties of earth masonry have been investigated in various researches such as Reddy, et al. (1989), Heathcote (1995), Bahar, et al. (2006), Jayasinghe, et al. (2009) and Sapir, et al. (2011). However, still there is less attention on their seismic performance under low to severe type earthquakes.

Among those natural disasters, unpredictability of earthquakes and their drastic impact make them as one of the most destructive natural disaster. According to EM-DAT International Disaster Database, earthquakes lost average about 27,000 lives per year since 1990. D. Guha-Sapir et al. (2011) listed and calculated the impact of ten most destructive earthquakes that happened within 1970-2008.

It is evident that the masonry buildings have not been designed for seismic loads when considering the true events occurred in Shensi in 1556, Haiyan in 1920, Kanto in 1923, Ashgabat in 1948, Pakistan in 2005 and Nepal in 2015 as stated by Balkhi (2016). In all these

events almost all the masonry buildings have collapsed leading to a death of more than 8,000 lives. Figure 1.1 clearly evident the severity of those above events.



**Figure 1.1: Damaged structures due to Nepal earthquake in 2015**

Therefore, there is a necessity of investigating seismic performance of masonry structures in regions of low to medium seismicity to enhance their seismic capacity.

## **1.2 Objective**

The main objective is to comparatively assess the in-plane and out-of-plane seismic performance of Cement Stabilized Earth Blocks (CSEB) and Cement Stabilized Rammed Earth (CSRE) walls with similar dimension via a series of shake table test and to recommend a most suitable numerical method for analysing the seismic performance of CSEB and CSRE walls.

## **1.3 Methodology**

First, a detailed literature review was carried out and also a market survey was undertaken on locally available earth masonry types, their sizes and locally available test apparatus and come up with suitable test specimen parameters. Second, a series of experiment for the selected parameters were carried out. Then, the numerical

predictions for experimental results were established. Finally, the most suitable computational software was recommended by validating with experimental results. Flow chart of the research methodology can be shown in Figure 1.2.

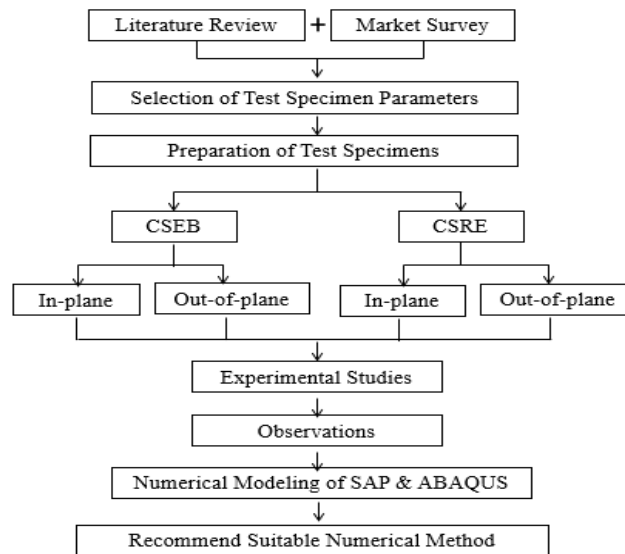


**Figure 1.2 : Flow Chart of Methodology**

#### **1.4 The Arrangement of the Thesis**

In this report the research project has been presented under six chapters. The first chapter contains the introduction, problem identification, objectives and methodology of the research.

Second chapter contains the details of past research studies done locally and globally relevant to the proposed research title and the research gap.

Third chapter contains the experimental studies while the fourth chapter discusses the analysis of experimental results.

Then, the fifth chapter contains the numerical modeling and prediction of experimental results.

Final chapter contains the conclusions and suggestions for future work relevant to the research topic.



## 2. LITERATURE REVIEW

### 2.1 Introduction

Much research regarding seismic performance of masonry structures either reinforced or unreinforced has been done locally and globally as in Figure 2.1. A few research works on the seismic performance of earth masonry structures have been done globally. There had been no attention on seismic performance of different type of earth masonry with locally available soil was done so far in Sri Lankan context nor worldwide. In this chapter it is discussed those above-mentioned research works to have a better awareness under the prevailing findings relevant to seismic performance of masonry structures.

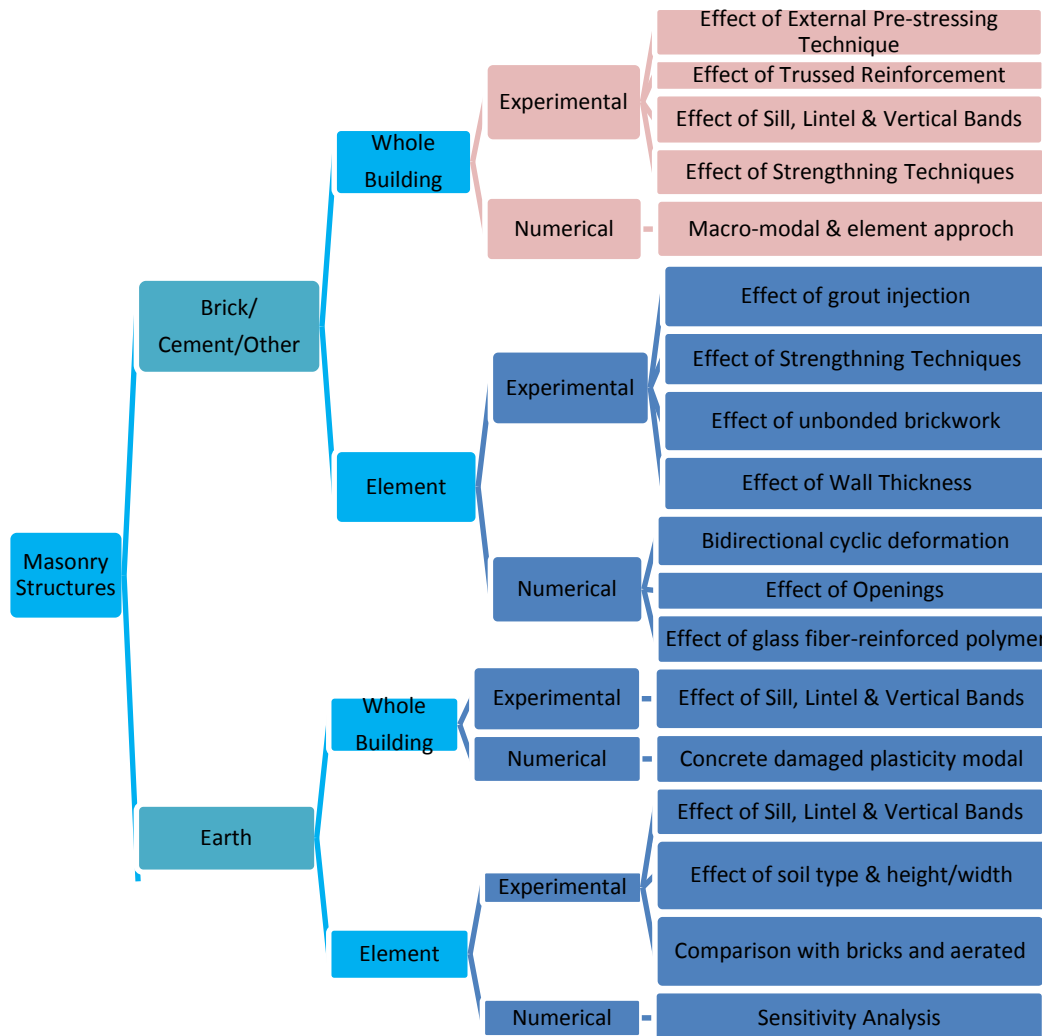


Figure 2.1 : Prevailing Studies relevant to Seismic Performance of Masonry Structures

## 2.2 Seismic Performance of Masonry Structures

### 2.2.1 Conventional Materials

Cole, et al. (2012) investigated the performance of brick veneer walls against out of plane loading which were subjected to in plane loading earlier. This was conducted by a shaking table test program on a full scale single room steel framed brick veneer house.

When constructing the house, it had been considered the general building practices in New Zealand and walls integrated with typical geometric features in different directions. The test house was subjected to different levels of El - Centro (EIC) earthquakes alternating from the moderate Serviceability Limit State (SLS) ground motion to design ultimate earthquake for New Zealand. Then the responses for each level can be compared with the minimum performance requirements specified in the New Zealand Earthquake Standard, NZS 1170.5 (2004). During the experiment following parameters were observed.

- Acceleration
- Drift
- Differential movements between steel frame and veneer



**Figure 2.2: Experimental set up with steel frames**

The test house as in Figure 2.2 resisted up to 2.6 times EIC with no brick loss and there were bricks loss at 2.7 times EIC due to severe rocking. These results showed that such type of construction would perform well better than the design seismic conditions in New Zealand.

Ma, et al. (2012) examined the performance of external pre-stressing technique for clay brick masonry structures under earthquake loads. The principle behind this technique is to locate the pre-stressing tendons on both sides of the walls and tensioning them to increase the in-plane shear strength and resistance of out-of-plane bending. In addition, this strategy enables multi-level pre-stressing at different floor levels of the structure along the building height. Shaking table tests for 1:4 scaled four storey house models were carried out for the validation of this technique. The external pre-stressing of masonry has improved the followings:

- Torsional resistance
- Flexural resistance of masonry walls and change the failure characteristics
- Energy dissipation capacity of the walls
- Overall stiffness of the masonry structure

Dolatshahi, et al. (2011) did a comprehensive numerical model with explicit computational procedures available in “ABAQUS” software. From this method, bidirectional cyclic deformation of masonry walls could be studied. The main objective of this study was to investigate the failure modes of unreinforced masonry walls for various loading directions. Bricks and mortar were modeled as solid 8-node brick element with reduced integration (C3D8R) and plane interface elements 8-node three-dimensional cohesive element (COH3D8) respectively. For the joints, elastic and plastic behavior was assumed. The failure modes for in-plane and out-of-plane loading were the diagonal crack and rocking mode respectively. The numerical model was validated with past experimental studies.

Meillyta, (2012) studied the performance of un-reinforced brick walls with openings under horizontal loads by developing load-drift relationship. In finite element method (FEM) “ABAQUS” software with explicit solver), continuum elements with inelastic behavior were chosen to numerically model the unreinforced masonry (URM) wall. The model was validated using the load displacement curve resulted from an experimental URM wall without openings.

Then a parametric study was conducted on the URM walls with openings under two different pre-compressive loads (i.e. 0.3 and 1.21N/mm<sup>2</sup>) as shown in Figure 2.3 to study the followings;

- Influence of area of openings
- Influence of pre-compressive load

on the horizontal load capacity of the wall. The results showed that horizontal load capacity;

- Decreases with increasing the area of openings
- Increases with increasing the pre-compressive load applied on the top of the walls.

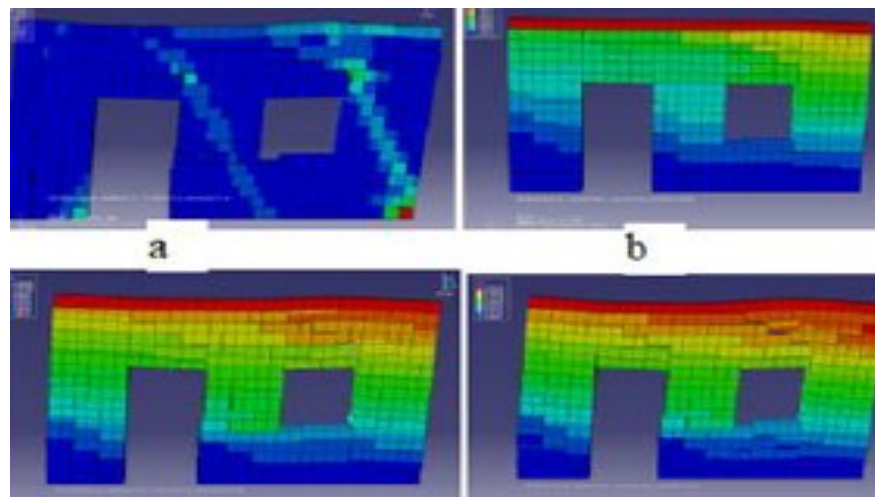


**Figure 2.3: FEM (ABAQUS with explicit solver with openings)**

Lourenco, et al. (2013) investigated the seismic performance of a new construction method using concrete block units and trussed reinforcement as in Figure 2.4 via a series of shaking table tests. Two geometrically identical two story 1:2 scaled models were prepared. One model was reinforced (RM) with the above new construction method and other was not reinforced (UM). Comparative parameters for experimental results were;

- Cracking patterns
- Failure mechanisms
- In-plane and out-of-plane displacements and lateral drifts

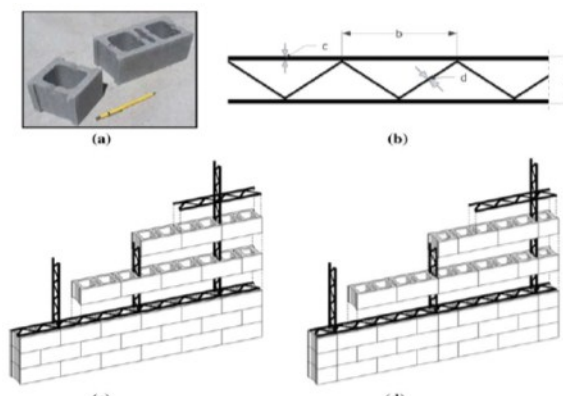


**Figure 2.4: New construction method with trussed reinforcement**

Behaviour factors for designing of un-reinforced masonry were also evaluated. The UM provided enough capacity for moderate and high earthquake loading while RM provided capacity for very high earthquake loading.

In RM cracks were visible at the first floor and on the masonry pier in between door and window opening.

In UM cracks were visible at both first and second floor levels and in the masonry piers. Crushing was in corner units and sliding movements along the bed joint crack and diagonal cracks.

Betti, et al. (2014) investigated the ability of estimating the seismic performance of unreinforced buildings among different numerical models and analysis methods. The experimental model of 1:1.5 scaled down two-storey building made from calcareous tuff stones with lime cement mortar was tested on the shaking table under increasing natural ground motions. The first numerical model and the second numerical model was built using macro-model (ANSYS) and macro-element (MATLAB) approach respectively. The main results of numerical and experimental studies have been compared. It has been reviewed that FE model is able to predict;

- Damaged areas
- Initial collapse mechanism

The macro element model can predict the collapse load accurately, but not the actual collapse mechanism. This method can be used only if the out-of-plane damage mechanisms are not initially activated. However, it can be fairly estimated the

fundamental dynamic response parameters by 6 degree of freedom models. Therefore, paper suggests following both numerical and analysis approach for the traditional and poor connected masonry buildings where global box behaviour cannot be assured.

Sivaraja, et al. (2013) evaluated the out of plane shear behavior of burnt clay brick masonry walls with and without glass fiber-reinforced polymer (GFRP).

Shock table tests on 1/3 scaled masonry elements (i.e. two elements with and without GFRP by the size of 1m x 1m x 0.092 m and 1m x 1.25m x 0.092m) were carried out by measuring the peak acceleration for each shock. Energy impact on wall by each shock was calculated using the velocity of impact and mass of the pendulum. It was found that energy withstanding of GFRP walls before the total collapse was about 18-24 times greater than walls without GFRP.

Silva, et al. (2014) experimental tests were carried out on 1:1 and 2:3 scaled multi leaf stone masonry panels which were in original conditions and strengthened with grout injections. The panels were subjected to horizontal in plane cyclic loading with vertical loading for different pre-compression levels. The objective of this study was to gather important information on static and dynamic behavior of three-leaf stone masonry structures in non-injected and injected conditions in terms of the followings;

- Failure mechanisms
- Maximum displacement capacity
- Shear strength
- Shear modulus
- Tensile strength, etc.

Non-injected panels went leaf separation at lower displacement levels while injected panels showed maximum resistance without any significant layer separation. And tensile strength and shear modulus increased by about 3 and 4 times respectively in grouted panels over non-injected ones. Hence this study has assessed and validated the effectiveness of injection of hydraulic lime-based grout as a reinforcement technique with the enhancement of displacement capacity, tensile strength and shear modulus.

Nayak, et al. (2016) investigated the efficiency of few strengthening techniques by following a series of shake table tests on many small-scale brick models (i.e. Free-standing walls, L- shaped walls and assembly of four walls). The strengthening techniques followed by authors were;

- Polypropylene (PP) band
- Vertical wire mesh
- L-shaped horizontal reinforcing bars
- Vertical reinforcing bars at corners

The behavior of each technique was compared under the crack patterns, failure behavior and overall effectiveness of the strengthening technique.

For free standing walls with all strengthening materials, the common failure was horizontal base shear. Among four methods, PP-bands showed the maximum strength improvement.

For L shaped walls, out-of-plane behaving walls are subjected to severe damage than in-plane behaving walls. And when the aspect ratio becomes 1:1, the strength can be improved at least 1.5 times from all strengthening techniques.

The experimental results showed that retrofitting materials alone or as a combination help to increase the strength, delay the failure and change the failure mechanism from brittle to ductile. Further, techniques which are cost effective and easy to implement were becoming more useful in enhancing seismic capacity. The results would be helpful to select the suitable retrofitting technique for a particular local condition.

Cakti, et al. (2016) built a 1:10 scale model of the 15th century Mustafa Pasha Mosque in Skopje, and followed shake table tests. The experimental results of various dynamic excitations were used for the calibration of the discrete element model in 3DEC which represents masonry mosque and minaret by rigid blocks interacting via contact elements as in Figure 2.5.

Then it was observed that numerical model can sufficiently simulate the time and frequency domain characteristics, damage regions and amount for lower level inputs.

Hence the discrete element approach can be used for the dynamic analysis of masonry structures which are relatively complex in laboratory conditions.

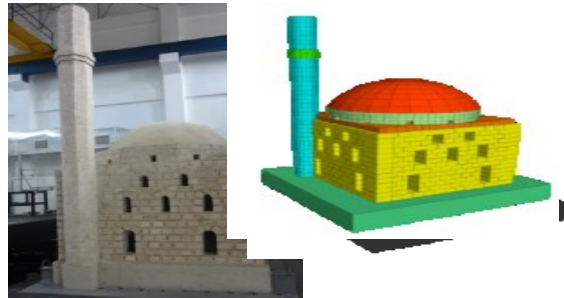


**Figure 2.5: Experimental setup and discrete model**

Palios, et al. (2017) one story and one bay steel frame in filled with un-bonded brickwork as in the Figure 2.6 subjected to in-plane and out-of –plane loading. Out-of-plane shake table tests and in-plane cyclic tests were carried out on the same wall specimen.

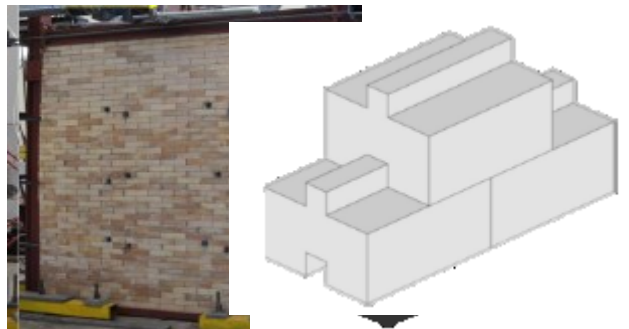


**Figure 2.6: Un-bonded brick work and interlocking masonry unit**

The damage was limited after cyclic in-plane inter-story drifts of 5.7%, due to hard contact of few bricks near the panel corner with columns. In the out of plane shaking, panels having a slenderness ratio of 22.5 was stable against 0.3g transverse acceleration and it collapsed when the weight of the wall acted outside the support.

Saleem, et al. (2016) studied the seismic response of brick houses which are retrofitted by different materials under shake table tests. Tests were performed on 1:4 scaled models such as;

1. Unreinforced Masonry model
2. PP-band model



3. GFRP retrofitted model
4. GFRP+PP-band retrofitted model (In this model, the minimum reinforcement ratio (0.0006) of GFRP was used as it is an expensive material).

In each model the damage initiation is from the openings to the corners and the observations of each model are described in the following Table 2.1.

**Table 2.1: Observations of each model**

Model	Observation
1	Highly brittle model and difficulty withstands even a small input motion.
2	Able to withstand a severe ground motion leading to intense cracking with separation of wall segments.
3	Sudden collapse without any early warning.
4	Increased ductility, remained serviceable even for a higher input of 1.2g and 5Hz, increased shear capacity and energy dissipation.

Finally, it was concluded that the combination with GFRP and PP-band is the best alternative against seismic loads as it enhances the shear capacity, energy dissipation and ductility considerably for an affordable retrofitting cost. And when using GFRP, it is required to use higher surface area at the bottom than the top as the failure (de-bonding of GFRP) begins from the bottom and moves top.

Nezhad, et al. (2016) investigated the performance of retrofitted brick walls using FRP against out of plane earthquake loads. Three I shaped 1:2 scaled walls were prepared, tested using one degree shaking table and a numerical model in “ABAQUS” software was also done as shown in Figure 2.7.

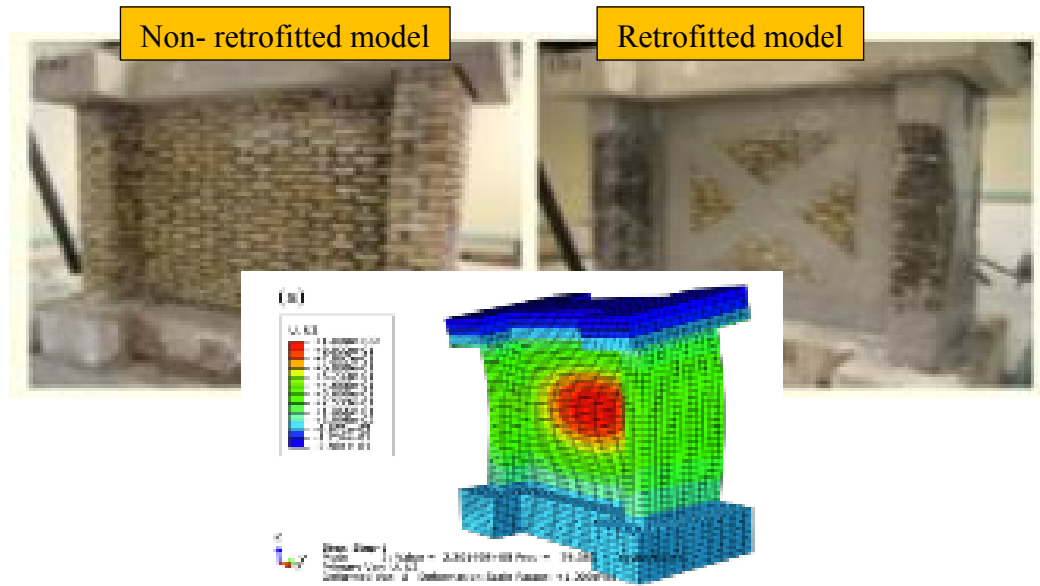


**Figure 2.7: Non-retrofitted and retrofitted walls and the numerical model**

In preparation of the walls, two transverse walls were used to prevent the overturning of the main wall against out of plane loads. Each wall was axially loaded with a concrete beam to simulate the scaling effect. The dynamic response of walls was reviewed under fundamental frequency, displacement, shear strength, crack patterns and energy absorption.

Experimental results discovered that FRP reinforcement can improve the shear strength and energy dissipation of masonry walls significantly.

In the un-reinforced specimen damage appeared throughout the height and in reinforced specimen only a major crack line occurred at the base.

Sanchez, et al. (2017) compared the numerical solutions with experimental results obtained from ceramic masonry walls subjected to compression and shear strength.

1:1 scaled physical models were prepared for 26 and 45cm thicknesses using solid masonry bricks with cement and lime mortar. In the numerical model, mortar joints were considered as interaction surfaces representing the behavior of mortar and masonry elements as a union shown in Figure 2.8.

In this report they have introduced;

- Strengths and weaknesses of adopted numerical modeling method

- Desirability of developing models that simulate the behaviour of great thickness masonry.

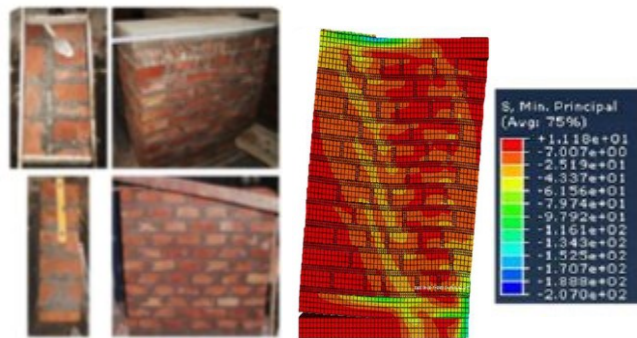


**Figure 2.8: Experimental wall and the numerical model**

### 2.2.2 Earth Materials

Tarque, et al. (2012) studied the non-linear dynamic behavior of adobe structures with numerical analysis since the limitations of experimental studies. The numerical model was validated with the experimental studies done at the Pontificia Universidad Católica del Perú by Blondet, *et al.* (2006).

The concrete damaged plasticity model in Abaqus/Explicit program was used in which the adobe was considered as an isotropic material. Further the adobe masonry can be considered as a homogeneous material because adobe and mortar are basically made of mud.

The elastic and inelastic material properties were obtained from an in-plane cyclic test carried out on adobe walls by authors previously.

The numerical model was subjected to a base acceleration recorded in the experimental studies. The numerical model was validated fairly well with the experimental results on the followings;

- Crack Pattern
- Failure Mechanism
- Displacement Response

The poor connection between the wooden beams of the roof and the adobe walls was simulated by reducing the element length, to avoid the physical connection at the wall corners. Figure 2.9 shows the experimental and numerical model respectively.

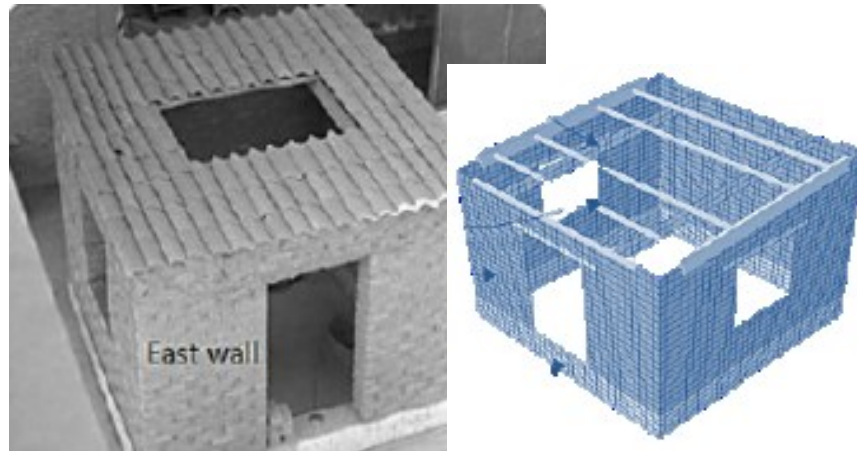


**Figure 2.9: Experimental and numerical model**

Keshav, et al. (2013) did a shaking table study for two reduced scale (1:3) single story masonry building models with hollow compressed stabilized earth block. One model was with earthquake resistant features (EQRf) such as sill, lintel and vertical bands and the other was without EQRf. In order to examine the seismic capacity of models, they were subjected to harmonic acceleration with gradually increasing amplitude until failure. Accelerations at plinth, lintel and roof level were recorded. The maximum accelerations imposed at roof level were 0.8512g and 0.6502g in models with and without EQRf respectively. The experimental study showed that the model with EQRf has better seismic resistance than the model without EQRf due to the joint action of masonry walls and their confining elements. The overall construction cost was increased by 4-6% due to adoption of EQ resisting bands.

Ratnam, (2014) has analysed dynamic behaviour of masonry wall panel of 1m×1.8m with an opening made out of hollow cement stabilized soil interlocking blocks. Two masonry walls with and without reinforcement (sill and lintel band and vertical reinforcement) were tested to determine their in plane cyclic performance. Lateral force was provided by a hydraulic actuator mounted horizontally at the height of the top surface of the wall. Lateral load and lateral displacement were measured. Also, numerical models using Structural Analysis Program (SAP 2000) have been done for

reinforced and non-reinforced block walls and bamboo walls as well. It was found that lateral resistance and ductility of masonry walls are improved by reinforcement.

Illampas, et al. (2014) calibrated and validated a numerical model for adobe masonry 1:2 scaled building which was subjected to horizontal loading using a hydraulic jack as in Figure 2.10. The displacements were measured at the upper section of the rear wall, the façade and the side wall. From the experimental studies following were realized:

- Initiation and Propagation of cracking failure.
- Damage limit states at different levels of deformation



**Figure 2.10: Load application using hydraulic jack**





Also, experimental results reviewed that adobe masonry structures subjected to horizontal loading are affected critically due to weak bonding between mortar joints and masonry units and lack of effective diaphragmatic function at roof level. Stress augmentation at the corners of openings and abutments of timber members was affected to the initiation of the damage. Further the occurred cracks closed completely, leaving a damage indication with the removal of applied loads and they open again with re-applied loads. This observation reminds that an adequate inspection of earthen structures should be carried out after seismic events.

According to the experimental data, a 3D FE model was developed in Abaqus/CAE and calibrated with force-displacement response and failure mode. An isotropic damaged plasticity constitutive law was adopted for numerical simulation. The FE

analyses revealed that the global structural behaviour was affected by assigned tensile response to the masonry medium and the structural behaviour of adobe masonry buildings subjected to horizontal loading can be sufficiently predicted. For further investigation on the dynamic performance of adobe structures, the calibrated FE model was subjected to a time history analysis of a real earthquake.

Srisanthi, et al. (2014), observed that when comparing the seismic capacity of scale 1:3 of single room houses made by burnt clay bricks, solid stabilized earth blocks, hollow stabilized earth blocks and modified stabilized earth blocks with and without EQRF, earth blocks behave better than bricks against long period ground motions. Collapse frequency of each model was as given in Table 2.2.

**Table 2.2: Collapse frequencies for single room models with different blocks**

Block Type	Collapse Frequencies
	X Hz
	2 (Burnt Clay Bricks of 76mm×36mm×25mm)
	1.77(Hollow Stabilized Earth Blocks of 140mm×70mm×50mm with 10% hollow)
	1.8(Solid Stabilized Earth Blocks of 140mm×70mm×50mm)
	2.259(Modified Stabilized Earth Blocks of (80mm×80mm×35mm)

Yaan, et al. (2016) investigated the seismic performance of rammed earth structures with and without a retrofitting technique by conducting series of shake table tests. Two full scale single floor one room models were constructed with locally available

soil while representing the local earth dwelling in China. The adopted retrofitting technique was externally and internally bonded tarpaulin fibre strips. Two models were subjected to east-west component of the El-Centro wave of progressively increasing intensities until model reached the failure condition. They observed changes in damages, deformation, dynamic properties and roof-wall interaction in the models. It was revealed that proposed technique can effectively improve the load bearing capability, structural stiffness and integrity of the building.

Lorenzo, et al. (2017) analysed the efficiency of structural elements in rammed earth with adopting a new strengthening system of polyester fabric strips under pseudo-dynamic loading. In-plane cyclic tests were carried out for strengthened and un-strengthened rammed earth walls and results were analysed in terms of viscous damping, stiffness degradation and energy consumptions. The strengthening system contributes to enhance displacement and horizontal load capacity while limiting the spread of cracking in un-strengthened walls.

Nabouch, et al. (2016), investigated the in-plane seismic performance of RE walls of two different height/width ratios and soil types. Walls were subjected to pushover tests and established the capacity curves. Walls with very stiff soil where shear wave velocity  $>800\text{m/s}$ , have an acceptable performance for seismicity zones from "very low" to "medium" while walls with good soil where shear wave velocity is  $300\text{m/s} - 800\text{m/s}$  have an acceptable performance for seismicity zones from "very low" to "moderate".

Mehmet, et al. (2017) observed the behaviour of rammed earth walls compared to masonry brick and aerated concrete walls under reversed lateral cyclic loading.  $20\text{cm} \times 150\text{cm} \times 150\text{cm}$  non-stabilized and stabilized (i.e. 10% stabilized, 10% cement stabilized with 1% glass fibres and 5% cement stabilized with 5% blast furnace slag mixtures) RE, brick and block walls were cast. Structural performances of above five types of walls were compared under load carrying capacity, total energy dissipation and stiffness degradation. Finally, it was found that stabilized (10% cement) RE walls show the better structural performance compared to others.

Kai, et al. (2015) proposed a retrofitting technique for RE walls to strengthen the seismic capacity. A tarpaulin with an NF compound was selected among two other different fibre materials, considering cost and reinforcement effect. Four full scale rammed earth walls of 2400mm×2100mm×600mm were built and three of them were reinforced using three different strengthening techniques. All the walls were subjected to in-plane shear loading and found that proposed retrofitting technique significantly increases the lateral load capacity and maximum horizontal displacement up-to 38% and 75% respectively.

Lorenzo, et al. (2016) performed a sensitivity analysis for the finite element model developed using DIANA software and calibrated it with the experimental results obtained from rammed earth walls subjected to cyclic loading. The behaviour of RE walls were simulated using total strain rotating crack model and Mohr-Coulomb failure criterion was used to simulate the interfaces between layers. The sensitivity analysis revealed that interface tensile strength and friction angle are the main parameters affecting to the shear behaviour while cohesion and layer thickness affect partially. Further, they mentioned that above results are related with a situation where considerable compressive stress is applied.

Table 2.3 illustrates the summary of few past research studies that have been conducted locally and globally relevant to the seismic performance of masonry structures.








**Table 2.3: Summary of few experimental and numerical research studies carried out relevant to the dynamic performance of different masonry structures**

Year	Country	Experimental			Numerical		Block Type and other materials/features	Full Scale	Reduced scale	House	Wall
		Shake Table	Shock table	Hydraulic jacks	Implicit/Explicit	Other					
2010	Australia						Bricks & Steel Frame				
2011	China						Bricks & Pre-Stress Tendons		1:4		
	USA				Abaqus /Explicit		Bricks				
2012	Indonesia				Abaqus /Explicit		Bricks				
	Italy				Abaqus /Explicit		Adobe				
	Portugal						Concrete/ Trussed Reinforcement		1:2		
	Iran				Find Properties for numerical modelling		Bricks				
	India						HCSE Blocks with & without EQRF		1:3		
2013	Italy					Macro & Micro Element Approach (Ansys)	Calcareous tuff stones		1:1.5		
	India						Bricks with GFRP		1:3		
	Italy						Stone Masonry with grout injections		2:3		
2014	Sri Lanka					SAP Analysis	Hollow cement stabilized soil interlocking blocks				
	Cyprus				Abaqus/CAE		Adobe Masonry		1:2		
	India						Bricks with PP bands, r/f bars, wire mesh		1:3 - 1:4		
	India					FEM by (Ansys)	Bricks and CSE blocks with and without EQRF		1:3		
2015	Turkey					Discrete Element Model in 3DEC	Stone & Brick		1:10		
	Greece						Bricks & Steel Frame				
	Japan					Applied Element Method	Bricks & PP bands & FRP		1:4		
	Iran						Brick & FRP		1:2		
2017	Argentina				Abaqus (Mortar Joints as interaction Surfaces)		Bricks				

### 2.2.3 Observed trends in dynamic performance of masonry structures through experimental studies

- Under dynamic loadings, URM experience cracks at each floor level along the height, crushing of corner units and sliding movement along the cracks. Initiation of damage is from openings to corners as stress augmentation at corners of openings.
- Under dynamic loadings, models with EQRF such as reinforced concrete bands at plinth, sill and lintel levels and vertical ties at door and window corners and sides behave better than models without EQRF as they improve the integrity of structure.
- Retrofitting materials such as FRP, PP bands and wire mesh can enhance the tensile strength, shear modulus, displacement capacity and delay the failure time and change the failure mode of the structure from brittle to ductile. Common failure with all above materials was the horizontal base crack.
- When comparing the results of three different experiments done for performance of masonry structures retrofitted with FRP same failure pattern can be observed as mentioned in Table 2.4.

**Table 2.4: Experimental results for different elements retrofitted with FRP**

	<p>-No damage within the Peak Ground Acceleration (PGA) range of 0.058g – 0.203g            -Crack initiation at PGA of 0.249 g            -Base Crack through the wall width</p>
	<p>-No damage within the PGA range of 0.05g – 0.20g            -Crack initiation at PGA of 0.4 g            -First diagonal cracks from wall opening corners and finally base crack</p>
	<p>-No damage up to 3.09g            -Crack initiation at PGA of 4.36 g            -Horizontal Crack above 20cm – 40cm height from the base of the wall</p>

- Further when using FRP, special attention should be given to the base as the appearance of major cracks and de-bonding of FRP initiates from the base.
- According to Srisanthi, et al. (2014), when comparing the dynamic performance of single room houses without EQRF made by burnt clay bricks, solid stabilized earth blocks, hollow stabilized earth blocks and modified stabilized earth blocks, modified earth blocks behave better than others.
- Seismic resistance of masonry structures can also be improved by increasing the pre-compression levels and reducing the opening areas.

#### **2.2.4 Summary of idealizations used in numerical modelling of masonry structures**

- Micro or macro modelling technique was used.
- Bricks and mortar were modelled using 8-node brick element with reduced integration (C3D8R) element or for the bricks, solid elements (C3D8R) together with or without plane interface elements 8-node three-dimensional cohesive element (COH3D8) for mortar between solid elements are used or each component of the wall were generated as head, horizontal joint, vertical joint, brick, half brick, bottom head and bottom slab.
- Bricks were expanded by half the mortar dimension in both directions as in figure 10.
- Bricks were divided into two parts for capturing the exact behaviour and crack propagation of the wall.
- Explicit solver in “ABAQUS” was chosen to model a URM wall as it is a computationally efficient and has low convergence problems over implicit method.
- They have been used either Drucker Prager plasticity model which can be used to model frictional materials or concrete damaged plasticity model which is developed for quasi-brittle materials subjected to cyclic loads in “ABAQUS”.
- Interaction between the bricks was modelled using normal and tangential behaviour interactions available in interaction module in “ABAQUS”.

- Static friction coefficient value of 5 and kinetic friction coefficient value in between 0.5- 0.75 were used in modelling.
- The bottom face of the masonry was restraint for all translating degree of freedoms.

Considering the all above studies carried out locally and globally, it was observed that dynamic properties of structural elements made from compressed earth blocks and rammed earth (stabilized/un-stabilized) have been investigated rarely with shake table tests followed by numerical studies. Hence in this study, the main objective was to comparatively assess the in-plane and out-of-plane seismic performance of CSEB and CSRE wall panles with similar dimension via a series of shake table test and then to recommend a most suitable numerical method for analysing the seismic performance of CSEB and CSRE walls.

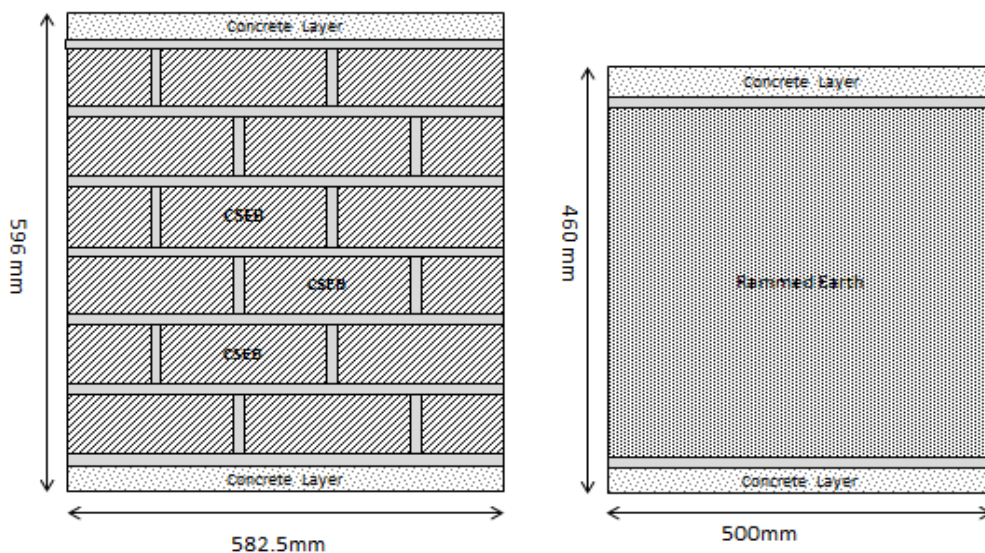


**Figure 2.11 : Wall panel sections selected for Research**

The dimensions of CSEB and CSRE wall panles were selected for the experimental studies according to the shake table payload capacity at Department of Civil Engineering, University of Moratuwa as illustrated in Figure 2.11.

At the same time two wall panels from each configuration were built in order to subject them in-plane and out-of-plane seismic loading.

During the parameters selection such as earth blocks, block pattern, soil type, panel thickness, compaction ratio, concrete layer thickness, etc it was considered the material availability, equipment capacities, expenditure on materials, construction in Sri Lankan context, easiness and practicability of construction and past research studies and design guidelines. Then only the findings of this research will be willing to adopt in construction industry.

### **3. EXPERIMENTAL STUDY**

#### **3.1 Introduction**

This section discusses the reasons and justifications behind the selection of parameters for experimental study and experimental results for each analysis.

#### **3.2 Selection of Parameters**

##### **3.2.1 Compressed Stabilized Earth Blocks Wall Panels**

Identical wall panels were constructed with solid plain CSEB of 225mm×110mm×75mm in size and stabilized with 6% cement. The bed joint was maintained as 10mm thick cement: sand mortar of 1:6 ratio. The dimensions of the specimen wall panels were selected based on the capacity of the shake table, which worked out to 582.5mm×110mm×596mm. A layer of 38mm thick, M15 grade concrete was placed at the top and bottom of each test panel to maintain the confinement of the element.

As indicated in Figure 3-1, the bottom concrete layer of the wall panel was fixed to the shaking table using four steel angle sections and twelve bolts. The test panels were fixed to the shaking table at each angle section by embedding one bolt in to the bottom concrete layer and two other bolts were used to connect the panels to the shaking table. For each material type, two identical panels were cast and tested under in-plane and out-of-plane loading.

Two wall panels having the same overall dimensions were built to subject them in-plane and out-of-plane seismic loading respectively as in Figure 3.1.

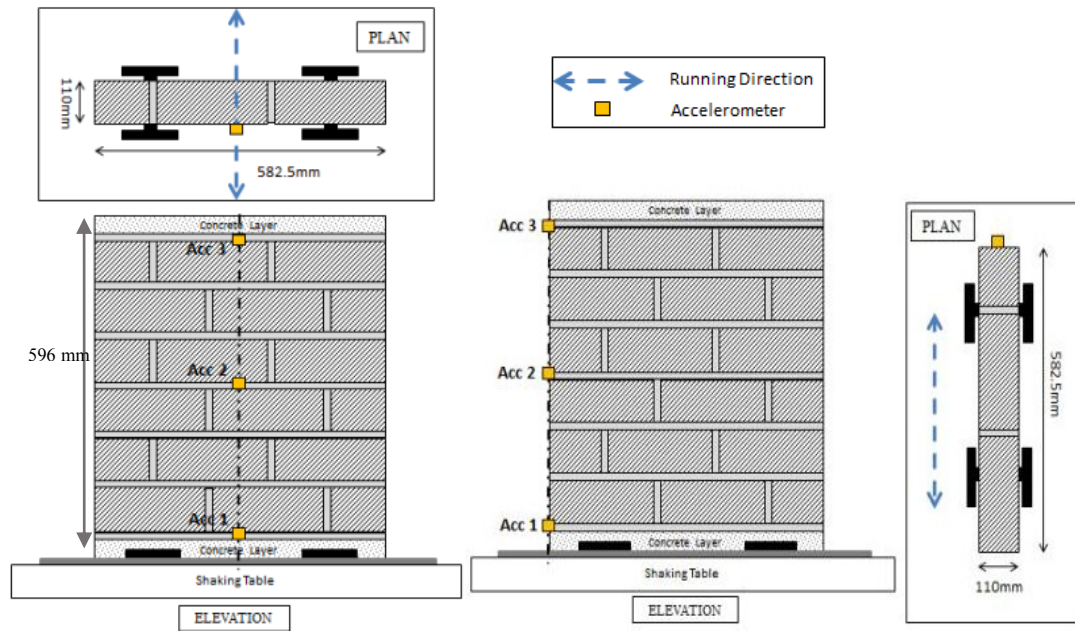


**Figure 3.1: Geometry of CSEB wall panels**

### 3.2.2 Rammed Earth Wall Panels

A suitable soil was selected for rammed earth walls with necessary soil testing. As reported in Jayasinghe, et.al (2007), laterite soil with 30% fines was used in RE specimen casting. Soil was stabilized with 8% of cement to achieve a higher strength and the water content was maintained by conducting the drop test to achieve an optimum density.

Keeping up with the capacity of the shake table, dimensions of the wall panels were limited to 500mm×150mm×460mm. A 38mm thick concrete layer of grade M15 was placed on top and bottom of each wall specimen for the confinement of the element.

A loose soil layer of 150mm thickness was compacted to have around 90mm thick layer using a 2.5kg pneumatic rammer (i.e. compaction ratio was 1.65).

As indicated in Figure 3.2, the bottom concrete layer of the wall panel was fixed to the shaking table using four steel angle sections and twelve bolts. The test panels were fixed to the shaking table at each angle section by embedding one bolt in to the



bottom concrete layer and two other bolts were used to connect the panels to the shaking table. For each material type, two identical panels were cast and tested under in-plane and out-of-plane loading.

Two wall panels having the same overall dimensions were built to subject them in-plane and out-of-plane seismic loading respectively as in Figure 3.2.

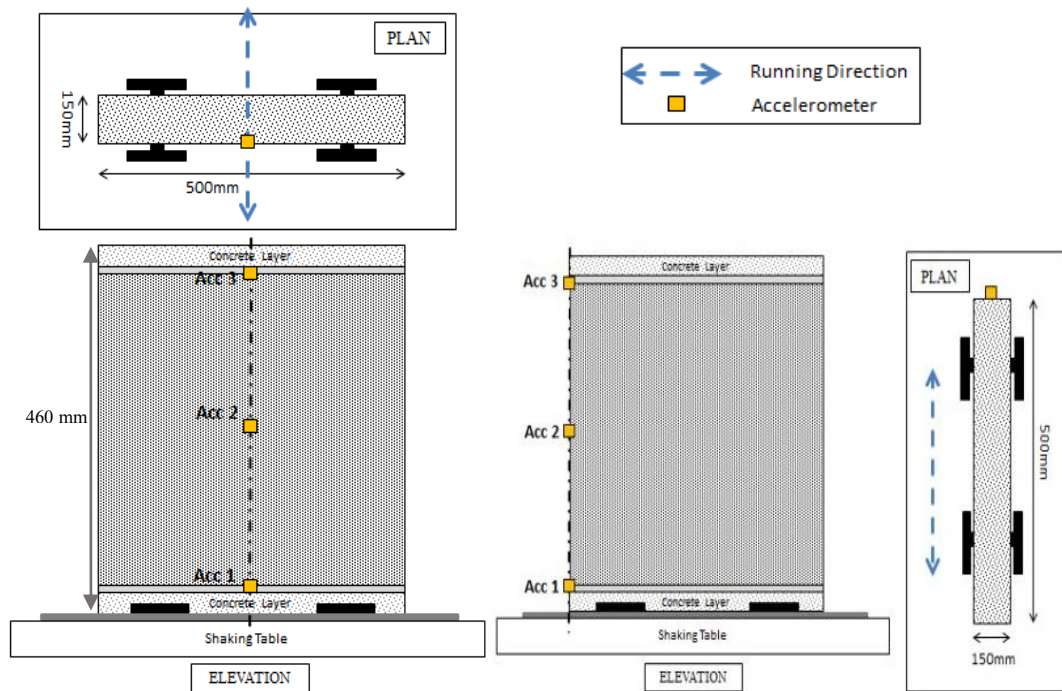


Figure 3.2: Geometry of CSRE wall panels

### 3.3 Material Properties

#### 3.3.1 CSEB

In order to assess the seismic performance of CSEB, solid plain blocks stabilized with 6% of cement were used. The key engineering properties of such CSEB were determined in the same experimental program.

This included the determination of average dry and wet compressive strength of CSEB sample which recorded as 6.3N/mm<sup>2</sup> and 2.5 N/mm<sup>2</sup> respectively. The

compression testing machine was used to test the blocks for compressive strength with the loading rate of 6.8kN/sec.

The sample of CSEB was tested for dry compressive strength by keeping the specimens in the oven for 24 hours and subsequently keeping under ambient condition for 24 hours. The wet compressive strength was determined by immersing the specimens in water for 24 hours followed by surface drying before testing.

Another important property is density of CSEB. The dry density of the blocks was determined after keeping the blocks in an oven for 24 hours. This has recorded an average value of 1830kg/m<sup>3</sup> for CSEB. The wet density of CSEB was determined by immersing block in water for 24 hours which recorded an average value of 2100kg/m<sup>3</sup>. Furthermore, the moisture content of CSEB was found to be in the range of 9.5%.

### 3.3.2 CSRE

Composition of the soil was determined by conducting the jar test in which one third volume of bottle was filled with soil and rest was filled with water. Then the sample was shaken and left for 24 hours and then the constituent can be found in separate layers. According to the jar test results the soil type was sandy clay as in Figure 3.3. Sandy clay soil was modified by adding sand and cement to become fine content of soil to 30% and 8% of cement for the preparation of walls.

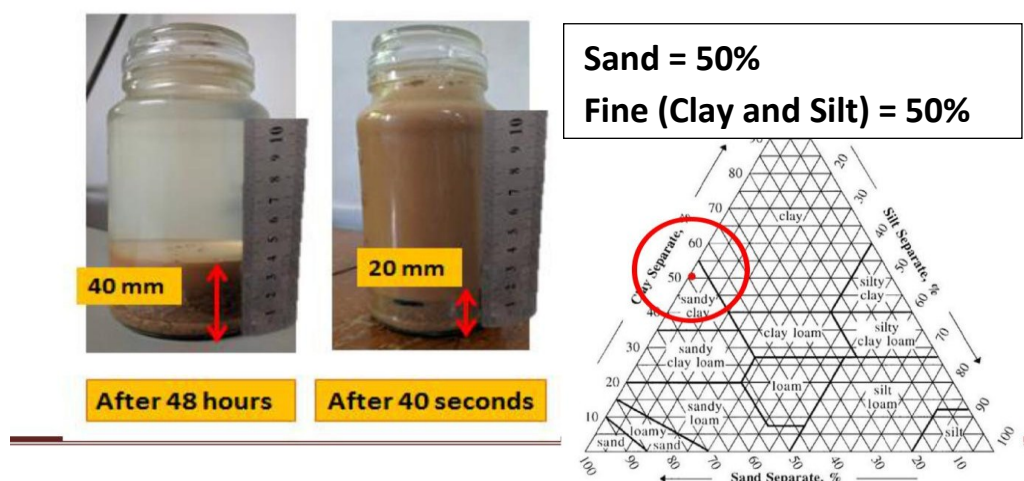


Figure 3.3: Jar Test

The optimum moisture content of the mix was maintained by conducting the drop test in which a ball of 40-50mm diameter was built using the palm and dropped it about 1m height. If the ball breaks in to four or five number of pieces, the added water content is sufficient enough.

Five cubes of rammed earth having 150mm×150mm×75mm dimensions were cast giving the same compaction ratio maintained in walls as in Figure 3.4. The compressive strength of those cubes were tested after one month of curing and got the value of 1.44N/mm<sup>2</sup>.



**Figure 3.4: Casting of CSRE cubes**

Further, the average wet density and dry density of CSRE was found to be 1927kg/m<sup>3</sup> and 1773 kg/m<sup>3</sup>.

### 3.4 Test Set Up

An experimental program was designed to investigate the seismic behaviour of earth masonry by simulating in-plane and out-of-plane loading. Wall specimens of CSEB and CSRE were tested on the shaking table in Figure 3.5 of one degree of freedom having a frequency range of 0-20Hz with peak ground acceleration of 1.5g. The table dimensions are 0.75m×0.5m. The maximum amplitude of deck displacement is 120 mm and the maximum pay load is equal to 80kg.



**Figure 3.5: Moratuwa University one-degree shaking table**

#### 3.4.1 Equalization

In order to achieve a higher reliability on seismic behavior, the input and output signals received and generated from the shaking table have to be equalized.

Equalization process should be carried out before starting the experiments. In this process, the drive signal imported to the shaking table with details of a known earthquake should be equalized with the output or feedback signal generated from the shaking table.

An accelerometer was attached to the shaking table and monitored the behavior with the known earthquake as the drive or input signal. The out-put or the feedback signal was observed and run for several iterations by varying the factors such as relaxation coefficient, average, high pass filter, low pass filter, etc until a close match is obtained for the drive and feedback signal.

The procedure of the equalization process is illustrated in Figure 3-6.



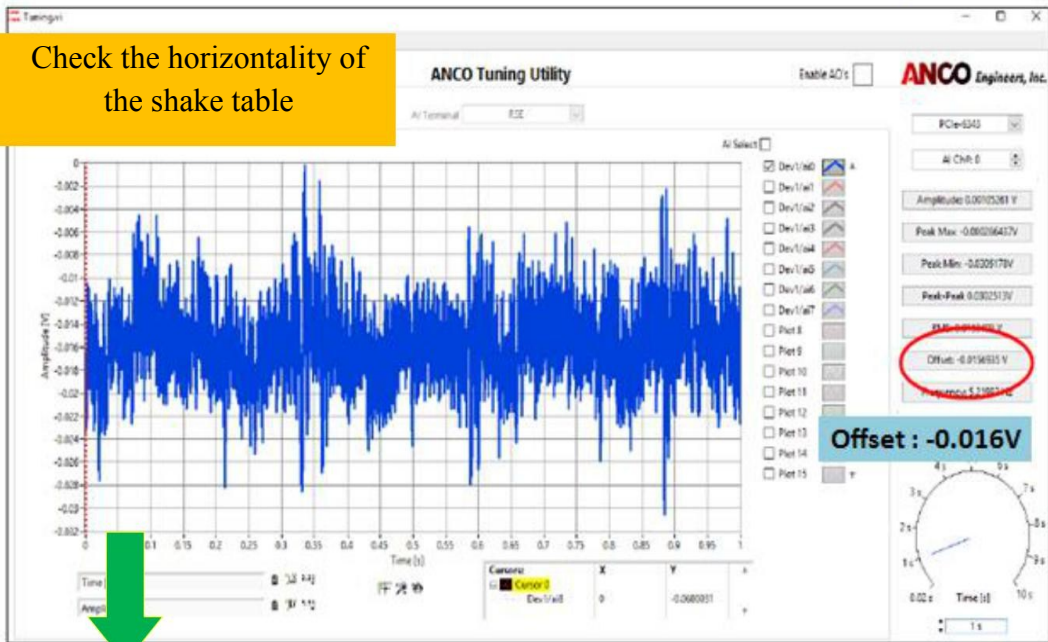
Fixing sensor to base

Setting sensor to channel board



Wave display in ANCO Tuning Utility

Check the horizontality of the shake table



**Importing Sensor Calibration Factor**

99.06 mV/G

The screenshot shows a software window with a menu on the left and a data table on the right. A yellow callout box highlights the 'Import' menu item. A blue callout box highlights the value '99.06 mV/G' in the table. A green arrow points from the menu to the table.

Channel	Unit	Cal. Coef.	Other 1
CH1	mV/G	99.06	
CH2	mV/G	99.06	
CH3	mV/G	99.06	
CH4	mV/G	99.06	
CH5	mV/G	99.06	
CH6	mV/G	99.06	
CH7	mV/G	99.06	
CH8	mV/G	99.06	
CH9	mV/G	99.06	
CH10	mV/G	99.06	
CH11	mV/G	99.06	
CH12	mV/G	99.06	
CH13	mV/G	99.06	
CH14	mV/G	99.06	
CH15	mV/G	99.06	

**Importing time history**

The screenshot shows a software window with a text editor on the left and a data table on the right. A yellow callout box highlights the text 'Importing time history'. A green arrow points from the text editor to the data table.

Time [s]	Value	Value	Value	Value
0	0.05500467	0	0	0
1	0.02	0.0317805	0	0
2	0.04	0.00864359	0	0
3	0.06	0.0373683	0	0
4	0.08	0.0661802	0	0
5	0.1	0.0949049	0	0
6	0.12	0.0595447	0	0
7	0.14	0.0241846	0	0
8	0.16	-0.0111756	0	0
9	0.18	0.0321297	0	0
10	0.2	0.075435	0	0
11	0.22	0.11874	0	0
12	0.24	0.0634736	0	0
13	0.26	0.00820705	0	0

**Checking limitations**

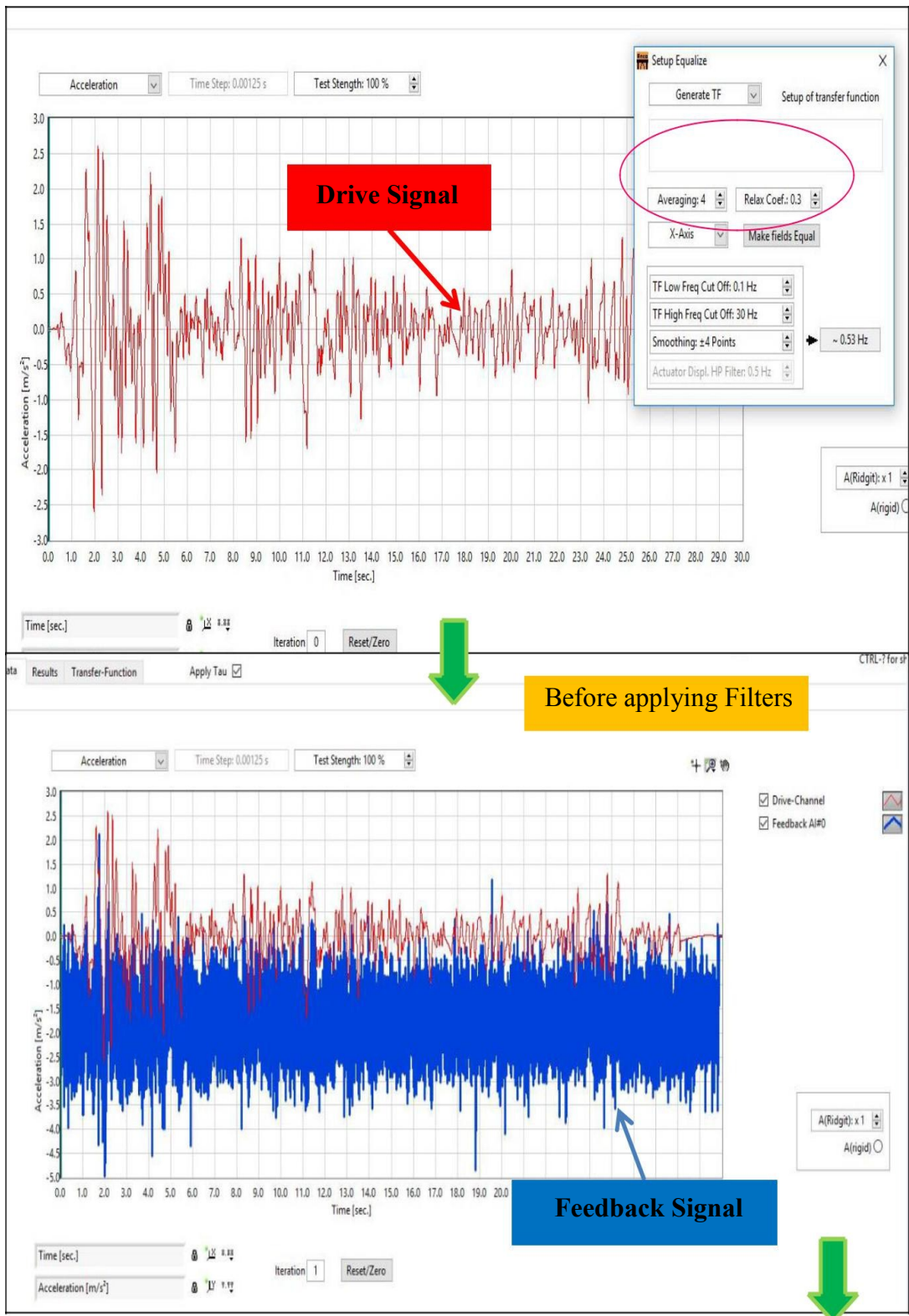
The screenshot shows a software window with a 'Import Text Time History' dialog box in the center, a graph of Acceleration [m/s<sup>2</sup>] vs Time [s] on the right, and a graph of Acceleration [m/s<sup>2</sup>] vs Frequency [Hz] at the bottom left. A yellow callout box highlights the 'Import Text Time History' dialog box. A green arrow points from the dialog box to the acceleration graph.

Import Text Time History

- Import System File
- Accel: 50 m/s<sup>2</sup>
- Vel: 2 m/s
- Displ: 0.2 m
- Pre DAC: 0 s
- Post DAC: 0 s
- Pre Rate: 100 #/s
- Post Rate: 100 #/s

Acceleration [m/s<sup>2</sup>] vs Time [s] graph shows a peak of approximately 2.5 m/s<sup>2</sup> at 10 seconds.

Acceleration [m/s<sup>2</sup>] vs Frequency [Hz] graph shows a peak of approximately 8.0 m/s<sup>2</sup> at 10 Hz.





Level/Target Data Results Transfer-Function Apply Tau

0 - Feedback C **Changing Filters**

Post Filtering Differentiate & Integrate

Global LP: 10.00 Hz  
Global HP: 1.00 Hz  
Hanning  Active

Low Pass and High Pass Filters

Load previous screen data

Ch#0	LP Filter: 10.00 Hz	HP Filter: 1.00 Hz	Hanning <input checked="" type="checkbox"/>	Active <input checked="" type="checkbox"/>
Ch#1	LP Filter: 10.00 Hz	HP Filter: 1.00 Hz	Hanning <input checked="" type="checkbox"/>	Active <input checked="" type="checkbox"/>
Ch#2	LP Filter: 10.00 Hz	HP Filter: 1.00 Hz	Hanning <input checked="" type="checkbox"/>	Active <input checked="" type="checkbox"/>
Ch#3	LP Filter: 10.00 Hz	HP Filter: 1.00 Hz	Hanning <input checked="" type="checkbox"/>	Active <input checked="" type="checkbox"/>
Ch#4	LP Filter: 10.00 Hz	HP Filter: 1.00 Hz	Hanning <input checked="" type="checkbox"/>	Active <input checked="" type="checkbox"/>
Ch#5	LP Filter: 10.00 Hz	HP Filter: 1.00 Hz	Hanning <input checked="" type="checkbox"/>	Active <input checked="" type="checkbox"/>
Ch#6	LP Filter: 10.00 Hz	HP Filter: 1.00 Hz	Hanning <input checked="" type="checkbox"/>	Active <input checked="" type="checkbox"/>
Ch#7	LP Filter: 10.00 Hz	HP Filter: 1.00 Hz	Hanning <input checked="" type="checkbox"/>	Active <input checked="" type="checkbox"/>
Ch#8	LP Filter: 10.00 Hz	HP Filter: 1.00 Hz	Hanning <input checked="" type="checkbox"/>	Active <input checked="" type="checkbox"/>
Ch#9	LP Filter: 10.00 Hz	HP Filter: 1.00 Hz	Hanning <input checked="" type="checkbox"/>	Active <input checked="" type="checkbox"/>
Ch#10	LP Filter: 10.00 Hz	HP Filter: 1.00 Hz	Hanning <input checked="" type="checkbox"/>	Active <input checked="" type="checkbox"/>

Note:  
No filters are applied until the Run button is pressed. This applies to all channels.  
All digital filters are Butterworth filters.  
Hanning is used for all channels.  
5% Hanning window is used for all channels.  
Drive function

Acceleration Time Step: 0.00125 Test Step

**Before applying Filters**

Acceleration [m/s<sup>2</sup>]

Time [sec.]

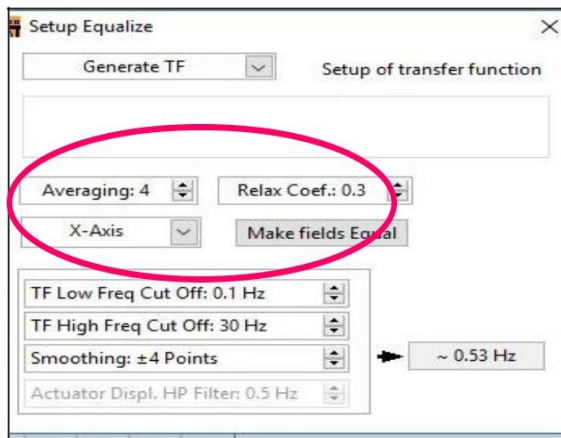
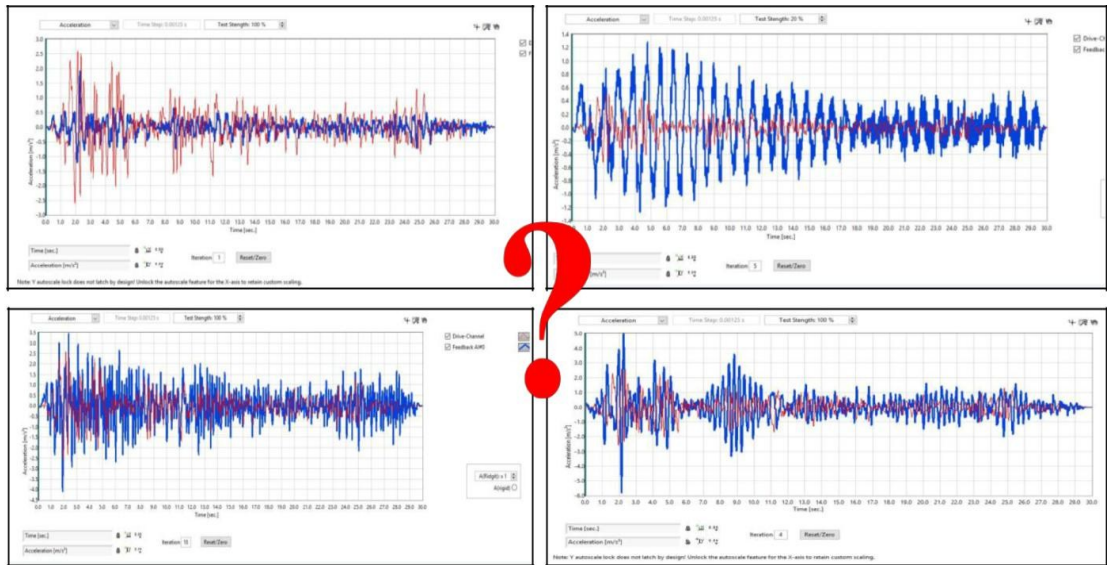
**After applying Filters**

Time [sec.] 0.00 0.01 0.02 0.03 0.04 0.05 0.06 0.07 0.08 0.09 0.10 0.11 0.12 0.13 0.14 0.15 0.16 0.17 0.18 0.19 0.20 0.21 0.22 0.23 0.24 0.25 0.26 0.27 0.28 0.29 0.30

Iteration 1 Reset/Zero

Note: Y autoscale lock does not latch by design! Unlock the autoscale feature for the X-axis to retain custom scaling.





Doing iterations with different,  
 - Averaging factors  
 - Relaxation coefficients  
 until there is a match between  
 both drive and feedback signals.

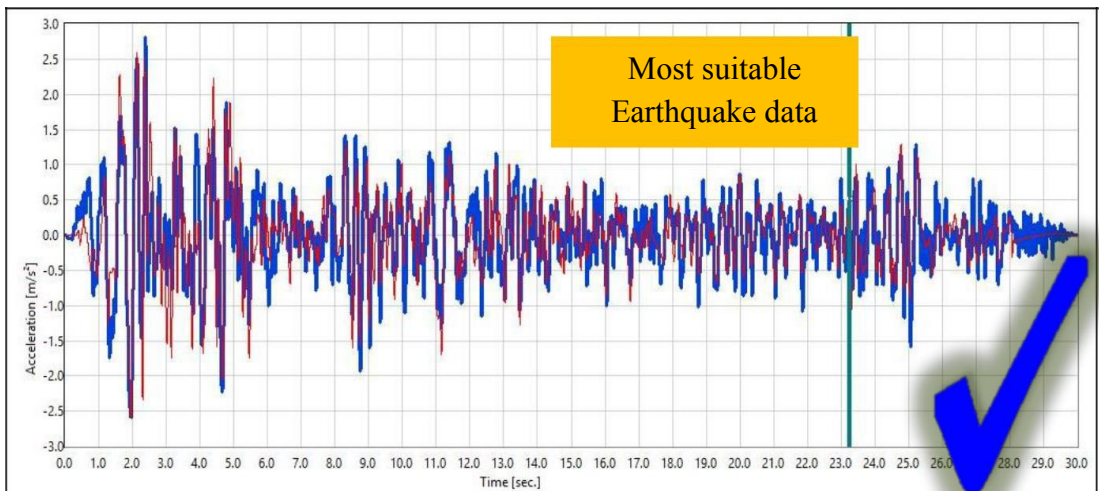


Figure 3.6: Equalization of Input and Output signals

### **3.5 Construction Sequence**

#### **3.5.1 CSEB Walls**

The half inch thick plywood board was cut to build the wall foundation as well as to fix it to the shake table. Then, the shake table hole pattern and wall orientation were marked on top of the plywood board and drilled relevant 10mm diameter holes for proper fixing the plywood board to the shake table. After that, four numbers of 25.4mm×25.4mm×150mm angle irons were cut and three number of 10mm diameter were drilled in each angle.

Two holes were on the horizontal plane of the angle for fixing the plywood board to the shake table. Other hole was on the vertical plane of the angle to mount the foundation anchor bolt. Then, four angles were placed and fixed to the plywood board using mounting bolts. Nails were fixed within the foundation area to have a firm bond between the foundation and the board. Having done that anchor bolts were fitted to the angles. Then 38mm thick M15 bottom concrete layer was laid as the foundation of the wall and cured for about 7 days.

Half thick block wall of 6 numbers of courses was constructed with 10mm mortar joints. While constructing the wall, steps were taken to place the sensor holders at the bottom, middle and top of the wall. Then, similarly to the bottom concrete layer, top concrete layer was also laid and the block wall was cured for 28 days. Finally, wall was painted with lime to identify the cracks during loading steps clearly.

This procedure was followed for both in-plane and out-of-plane walls.

The above described construction procedure is illustrated in Figure 3.7.



Figure 3.7: Construction steps of CSEB wall panel

### 3.5.2 CSRE Walls

The half inch thick plywood board was cut to build the wall foundation as well as to fix it to the shake table. Then, the shake table hole pattern and wall orientation were marked on top of the plywood board and drilled relevant 10mm diameter holes for proper fixing the plywood board to the shake table. After that, four numbers of 25.4mm×25.4mm×150mm angle irons were cut and three number of 10mm diameter were drilled in each angle. Two holes were on the horizontal plane of the angle for fixing the plywood board to the shake table. Other hole was on the vertical plane of the angle to mount the foundation anchor bolt. Then, four angles were placed and fixed to the plywood board using mounting bolts. Nails were fixed within the foundation area to have a firm bond between the foundation and the board. Having done that anchor bolts were fitted to the angles. Then 38mm thick M15 bottom concrete layer was laid as the foundation of the wall and cured for about 7 days.

Wood formwork was constructed as per the wall dimensions. It is a detachable type formwork with wooden bracing to avoid the buckling of wall during the compaction. The provisions were made to place the sensor holders. Oil was applied inside the formwork in order to avoid soil bonding to the formwork.

Next, 150mm thick CSRE wall was constructed by compacting four number of equal height soil layers. In other words, each 150mm height soil layers were compacted to around 90mm height using the rammer. While constructing the wall, steps were taken to place the sensor holders at the bottom, middle and top of the wall. Then, similarly to the bottom concrete layer, top concrete layer was also laid, and the block wall was cured for 28 days. Finally, wall was painted with clay to identify the cracks during loading steps clearly.

This procedure was followed for both in-plane and out-of-plane walls.

The above described construction procedure is illustrated in Figure 3.8.



All the specimens were constructed within the area closer to the shake table in order to facilitate safe transportation of the specimens on to the shake table.

Figure 3.9 shows the finished view of CSEB and CSRE wall panels after the application of lime and clay paint respectively.



Figure 3.8: Construction steps of CSRE wall panels



**Figure 3.9: Final view of wall specimens**

### **3.6 Sequence of Loading**

All the wall specimens were subjected to a set of selected seismic wave categories as indicated in Table 3.1.

As the first step, an actual earthquake (North-South component of 1940 El-Centro earthquake) was fed as an input with the ground acceleration to represent moderate, severe and the magnitude in between moderate to severe seismic levels. This is identified as category 1 in Table 3.1 which describes the loading process. Different severity levels of the seismic forces generated by El-Centro earthquake were established with the weightages recommended by Vidal, et.al (2012). El-Centro earthquake was occurred in southeastern Southern California near the international border of the United States and Mexico on May 18<sup>th</sup> of year 1940.

According to **El-Centro vibration data**, the acceleration vs. time values that was used for the shake table studies has been presented in a table up-to 2.8 seconds under the **Appendix A**. The full data list has been attached in a **CD as Appendix C**.

Upon applying different ground accelerations corresponding to three severity levels of seismic forces, the deflection and acceleration recorded in the specimen wall panels were measured at top, middle and bottom for each time increment of

0.00125s. Acceleration and displacement results obtained until 0.1 seconds for CSEB wall panel under in-plane loading of moderate sized earthquake have been presented in **Appendix B**. Acceleration and displacement results obtained for CSEB and CSRE wall panels under in-plane and out-of-plane loading from moderate to severe sized earthquake have been attached in a **CD as Appendix C**.

Alternatively, a sine wave was used to generate the seismic loads on the specimen wall panel, as stated in Nezhad et al. (2016), since there were no visible indications of damage in the specimen wall panels due to the actual seismic waves. As reported in Priyantha, (2016), the peak ground acceleration of 0.13g was selected as the first amplitude of the sine wave. Thereafter the acceleration and the frequency of the sine wave were increased progressively in steps of 2 as indicated in Table 3.1.

**Table 3.1: Loading Steps**

	Applied Wave	
Category 1	0.89 El-Centro	Moderate sized
	1.28 El-Centro	Moderate-Severe sized
	1.72 El-Centro	Severe sized
Category 2	0.13g×1 , (1 Hz)	Sine
	0.13g×2 , (2 Hz)	Sine
	0.13g×4 , (4 Hz)	Sine
	0.13g×6 , (6 Hz)	Sine

Since the shaking table is one degree of freedom, the test panels were placed parallel to the loading direction to simulate the in-plane behaviour whereas panels were placed perpendicular to the loading direction to monitor the out-of-plane behaviour. The loading direction and the orientation of the test panels were shown in Figure 3-10.

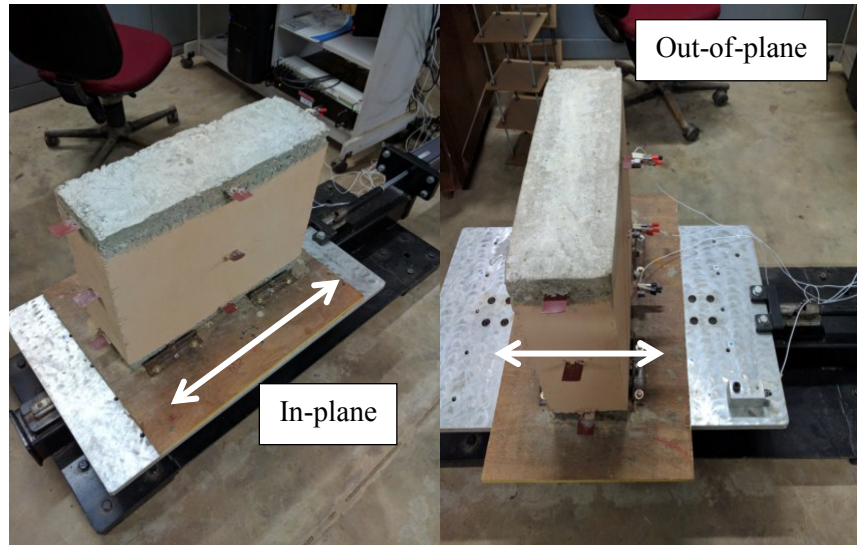


**Figure 3.10: Test specimens loading directions**

### **3.7 Summary**

The dimensions of wall panels were selected based on previous research and limited due to the shake table capacities. Two walls of each earth masonry type were cast and loaded them in-

plane and out-of-plane. The test panels were loaded under the two categories. The first category was an actual earthquake (North-South component of 1940 El-Centro earthquake) with three different scales and the second was a sine wave with four different frequencies and amplitudes.

The behavior of walls was studied in terms of displacement and acceleration response, base shear, failure magnitude and type.



## 4. RESULTS AND DISCUSSION

### 4.1 General

The structural behavior of specimen wall panels under seismic loads of different levels of severity is presented in sections 4.2 and 4.3 for CSEB and CSRE respectively.

### 4.2 Performance of CSEB Walls under Seismic Loads

As the first step the CSEB specimen wall panels were subjected to the category 1 wave respectively, three severity levels of El-Centro earthquake. There were no visible cracks observed in the wall panels. However, the variations observed in the sensors when the wave changes from moderate to severe are presented in Figure 4.1. The maximum displacement and acceleration recorded at the crest of the wall was taken into consideration.

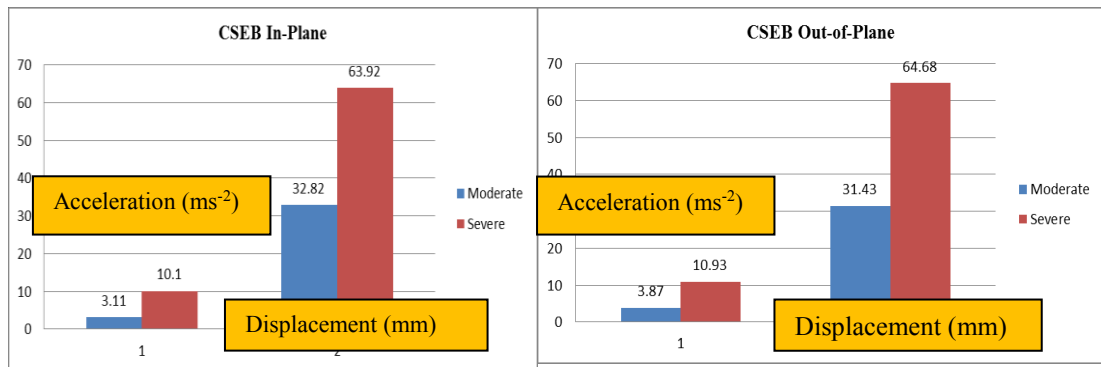
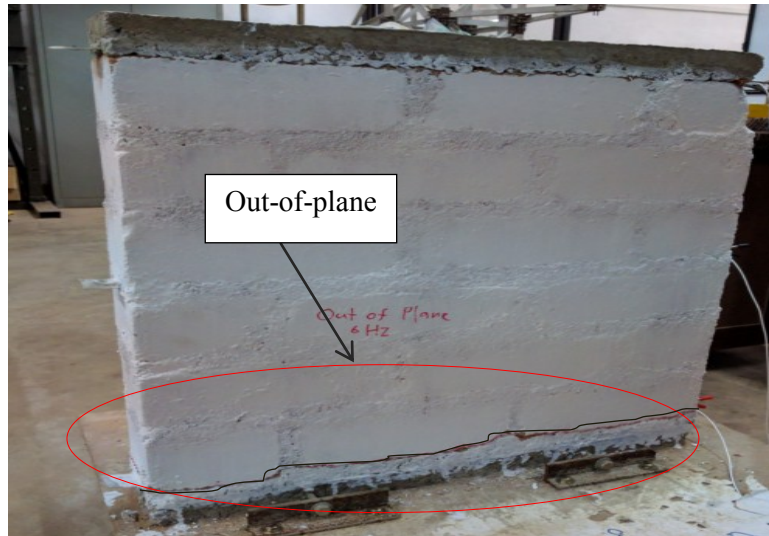


Figure 4.1: Variation of acceleration and displacement in CSEB panels

When the wall is subjected to the category 2 sine wave, following behavior was observed;

- i. There were no visible cracks observed for both in-plane and out-of-plane loading directions, until the frequency reached 4 Hz.
- ii. When the frequency of the wave becomes 6 Hz, a crack was formed at the base and propagated throughout the wall when the load application was in out-of-plane direction, as shown in Figure 4.2. However, no visible cracks were detected when the load was applied in-plane.



**Figure 4.2: Base crack in CSEB out-of-plane wall**

### 4.3 Performance of Stabilized Rammed Earth Walls under Seismic Loads

As the first step the CSRE specimen wall panels were subjected to the category 1 wave respectively, three severity levels of El-Centro earthquake. There were no visible cracks observed in the wall panels. However, the variations observed in the sensors are presented in Figure 4.3. The maximum displacement and acceleration recorded at the crest of the wall was taken into consideration.

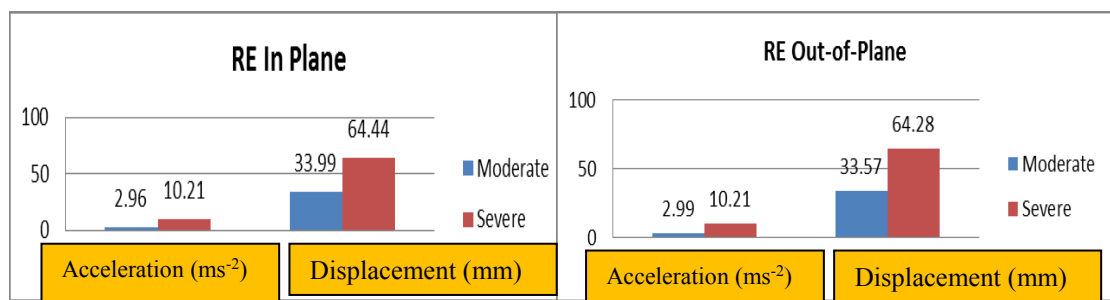


**Figure 4.3: Variation of acceleration and displacement in RE panels**

When the wall is subjected to the category 2 sine wave, following behavior was observed;

- i. There were no visible cracks observed for both in-plane and out-of-plane loading directions, until the frequency reached 4 Hz.

ii. When the frequency of the wave becomes 6 Hz, base crack was developed throughout the wall width with rocking mode in the out-of-plane wall and base crack was developed with some translation to the loading direction in the in-plane wall as in Figure 4.4.

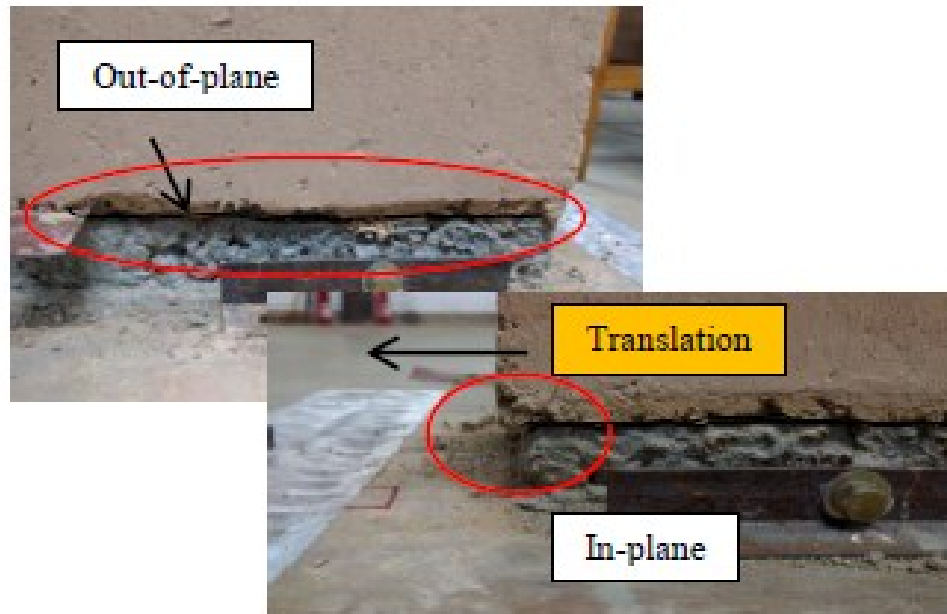


**Figure 4.4: Base crack in CSRE wall panels**

#### **4.4 Comparison of results**

Maximum acceleration and displacement at the crest of the wall and maximum base shear during the first loading category are illustrated in Table 4.1.

Further, the occurrence of visible cracks in earth walls during first and second loading category is indicated in Table 4.2.

**Table 4.1: Responses during loading category 1**

Wave Type	Maximum acceleration at crest of the wall (m/s <sup>2</sup> )	Maximum displacement at crest of the wall (mm)	Maximum Base Shear (kN)
CSEB In Plane			
0.89EI	3.11	32.82	0.24
1.28EI	3.79	46.57	0.30
1.72EI	10.10	63.92	0.79
CSEB Out-of-Plane			
0.89EI	3.87	31.43	0.30
1.28EI	4.53	37.16	0.35
1.72EI	10.93	64.68	0.85
CSRE In Plane			
0.89EI	2.96	34.00	0.19
1.28EI	3.82	39.22	0.25
1.72EI	10.21	64.44	0.65
CSRE Out-of-Plane			
0.89EI	2.99	33.57	0.19
1.28EI	3.74	38.89	0.24
1.72EI	10.21	64.28	0.65

**Table 4.2: Occurrence of visible cracks**

Observation of Visible Cracks				
	CSEB In Plane	CSEB Out-of-Plane	CSRE In Plane	CSRE Out-of-Plane
0.89EI	×	×	×	×
1.28EI	×	×	×	×
1.72EI	×	×	×	×
1Hz (0.13g×1)	×	×	×	×
2Hz (0.13g×2)	×	×	×	×
4Hz (0.13g×4)	×	×	×	×
6Hz (0.13g×6)	×	√	√	√

The maximum base shear was calculated by multiplying the effective mass of specimen with the top acceleration. Within the range of moderate to severe earthquake, base shear of CSEB out-of-plane wall was 7.6% higher than the in-plane wall and for RE walls, base shear was always similar for both types of walls as illustrated in Figure 4.5.

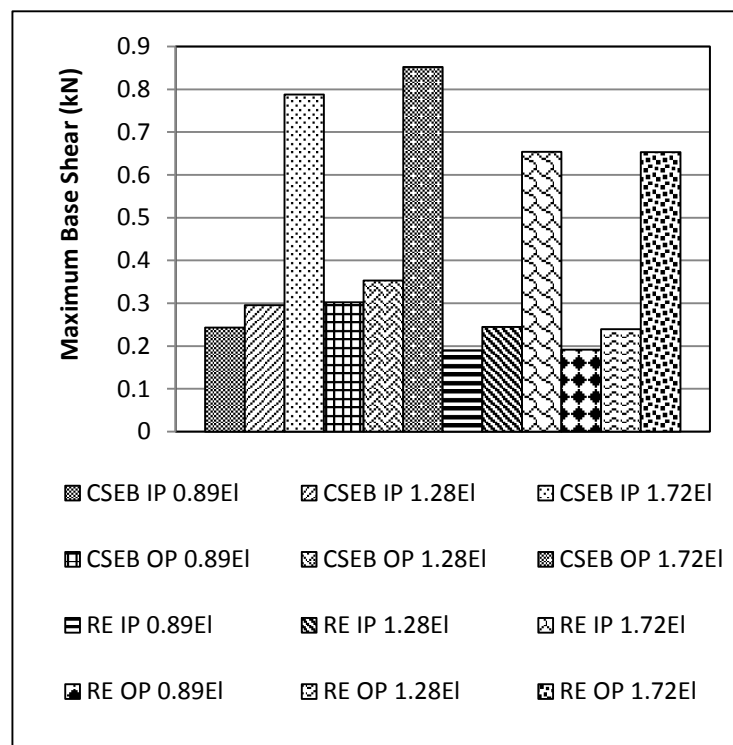


**Figure 4.5: Base Shear distribution during load category 1**

## 4.5 Summary

According to the experimental results from moderate to severe earthquakes, both CSEB and CSRE wall panels performed well without any visible cracks. In CSEB wall panels, maximum acceleration and displacement at the crest of the wall and base shear is 8.2%, 1.2% and 7.6% greater in out-of-plane loads than the in-plane walls under severe earthquake. But in RE wall panels those above considered values remain same for both in and out-of-plane walls.

In order to investigate the progressive damage behavior of earth walls, they subjected to sine waves with increasing amplitudes and frequencies. In CSEB walls, there were no visible cracks both in and out-of-plane walls until the 4Hz sine wave. But when the frequency become 6Hz, base crack was initiated and spread throughout the wall width in the out-of-plane wall and no visible cracks in the in - plane wall. In CSRE walls, there were no visible cracks both in and out-of-plane walls until the 4Hz sine wave. But when the frequency become 6Hz, base crack was developed through the wall width with rocking mode in the out-of-plane wall and base crack was developed with some translation to the loading direction in the in-plane wall. Tensile and shear failure at the base is the common failure type of out-of-plane and in-plane unreinforced walls respectively. Hence, strengthening should be carried out at the base of the walls.

## 5. NUMERICAL MODELLING

The dynamic properties of structural elements made from earth masonry such as rammed earth and compressed earth blocks (stabilized/un-stabilized), have been investigated rarely with experimental studies. Further to that, numerical studies with computer modelling have occasionally been carried out on earth masonry. Such numerical analysis will be made useful by validating with experimental results. So that more resource intensive and repetitive laboratory trials for varying types of masonry could be minimized.

In this paper, attention also has been paid for analysing alternative numerical models using two different computer software. Further the experimental data have been used to validate the numerical results and find their limitations.

Initially, the numerical modelling was started with Structural Analysis Program (SAP) and ABAQUS software. The experimental results of 0.89E1- Centro earthquake were compared with numerical results of SAP and ABAQUS in terms of displacement variation with time at the wall bottom, middle and top. According to the comparison, ABAQUS model was found to be the most recommended numerical model over SAP. Hence the numerical modelling was continued with ABAQUS for other loading steps as well.

Two different comparisons have been undertaken to validate the accuracy of the finite element model developed using the general finite element package ABAQUS.

- i. Verification for displacement vs. time under moderate to severe earthquake.
- ii. Verification of failure load and type under moderate to severe earthquakes and at the sine wave that caused the failure.

In this section, first the modelling steps of SAP and ABAQUS and their results under moderate earthquake have been illustrated. Then the above mentioned two different

comparisons in ABAQUS model have been demonstrated for moderate to severe and at the failure loading condition.

## 5.1 The Process of Numerical Modelling in SAP

The main steps of the dynamic analysis and the sequence of modelling the dynamic performance of CSEB walls using finite element software SAP have been illustrated in Figure 5.1.

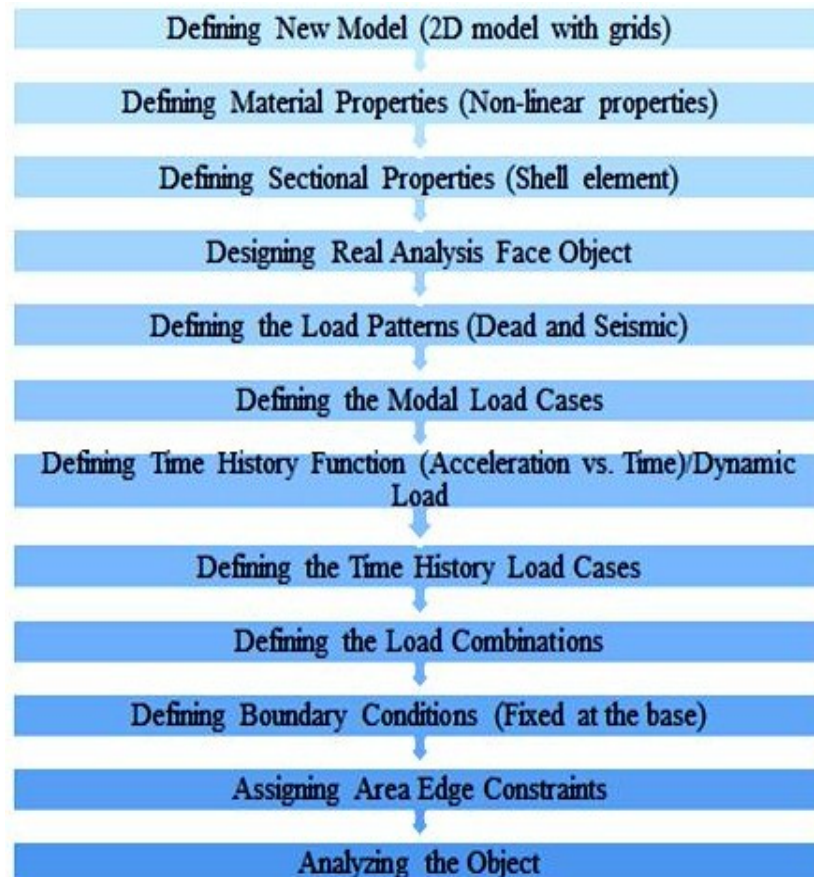
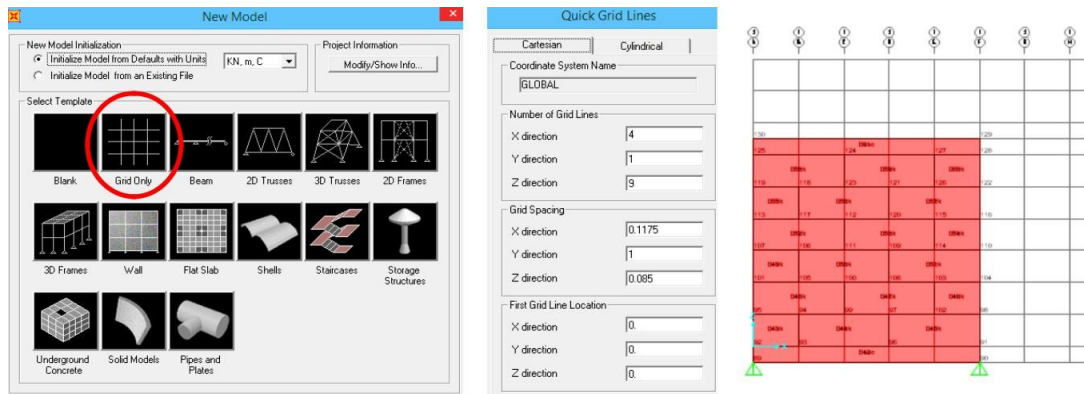


Figure 5.1: Steps in SAP model

### 5.1.1 Defining New Model

The numerical modelling was started with ‘Grid Only’ model type. Then the required number of grid lines and spacing were defined according to the dimensions of block unit, concrete layer thickness, mortar joint, number of courses and number of block units per course as in Figure 5.2.





**Figure 5.2: Grid type model**

### 5.1.2 Geometry

CSEB unit and mortar was modelled as a one unit by expanding the block by  $\frac{1}{2}$  mortar thickness in one or both directions according to Figure 5.3. The element type is shell thin element with membrane and bending thickness.

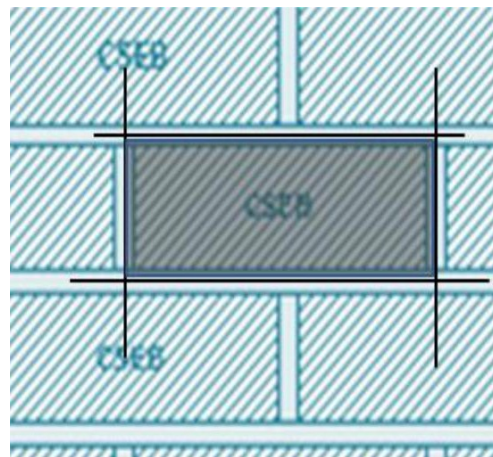


**Figure 5.3: Block and mortar as one unit**

### 5.1.3 Material Properties

General, elastic and plastic properties were assigned to the block and mortar assemblage. In this mechanical modelling, “Drucker Prager” plasticity model was considered as it can be used to model frictional and pressure dependent materials. Figure 5.4 shows the steps in defining material properties.

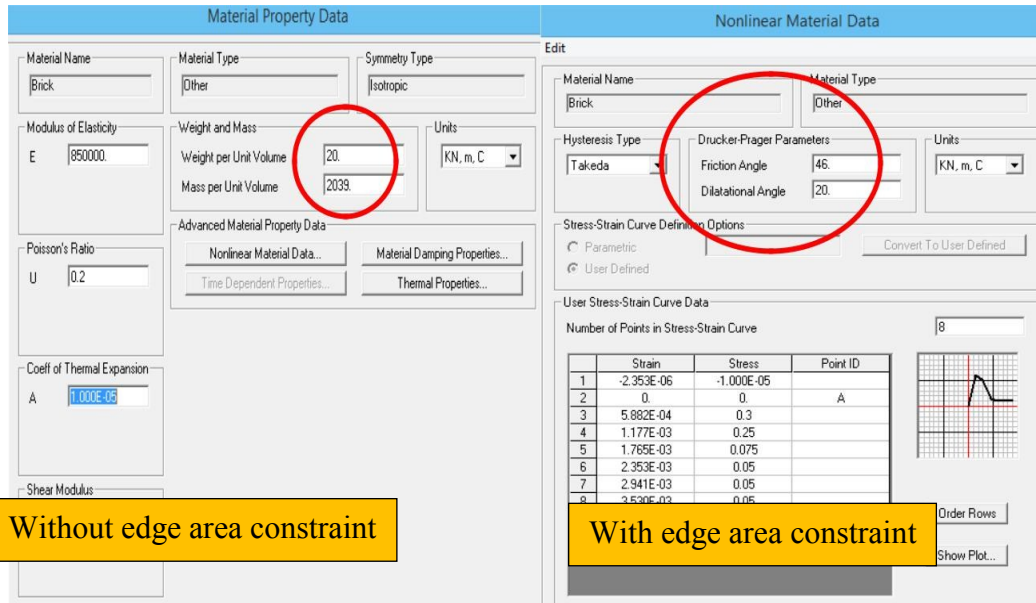


Figure 5.4 : Defining material propertie

### 5.1.4 Restraints

The blocks and concrete layer elements were arranged accordingly. Having done that, pin joints were assigned for the base and edge area constraint was applied for all block units to maintain slight displacement discontinuities. If the edge area constraint is not applied, the results and deformation of the structure is not realistic. The difference in the deformation of the model with and without edge area constraint can be seen in Figure 5.5.

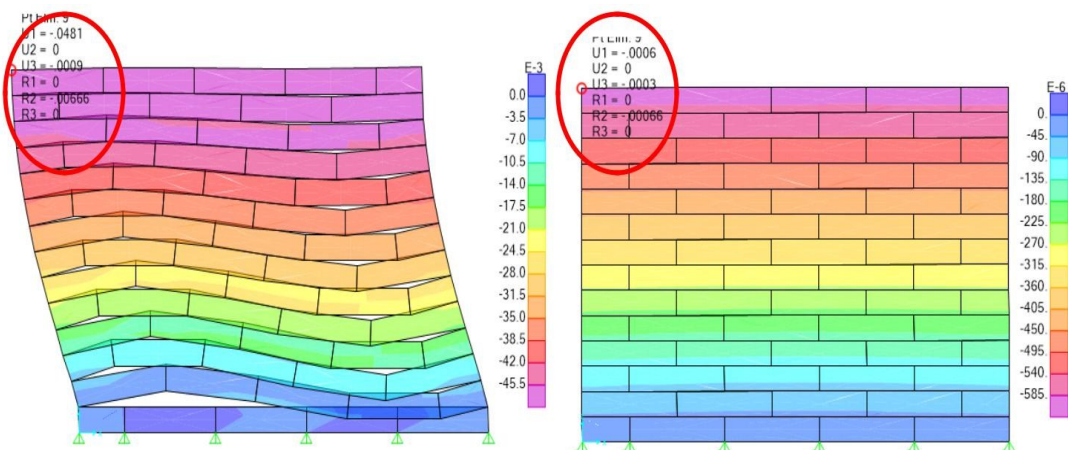
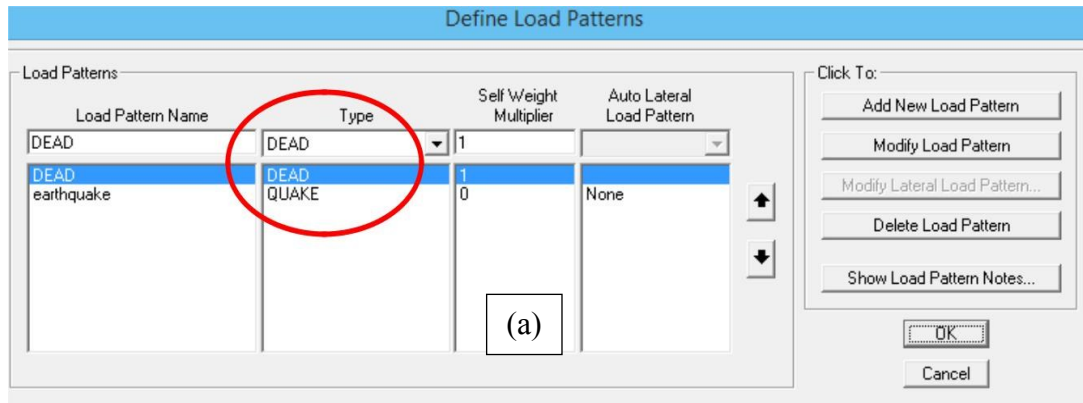


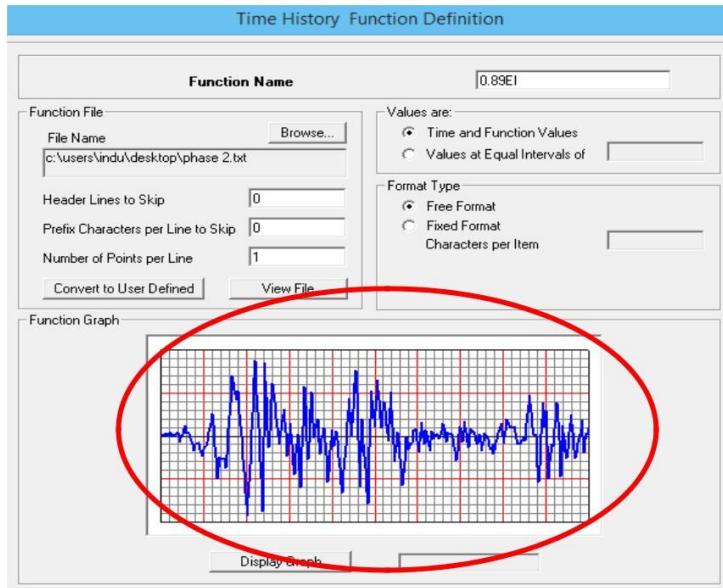
Figure 5.5: Effect of edge area constraint

### 5.1.5 Loading

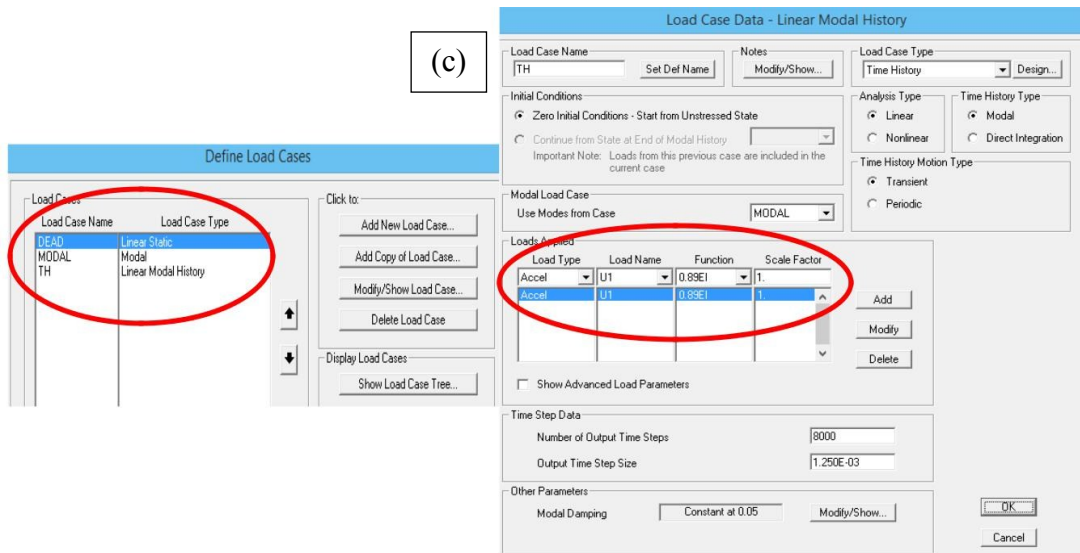
Loading was applied as acceleration with time. First, the dead and quake load patterns were defined. Second, the time history function for the moderate earthquake was defined using the „Function“ option. Then the dead, modal and time history load cases and one load combination of dead and earthquake were defined as in Figure 5.6.



(b)



(c)



(d)

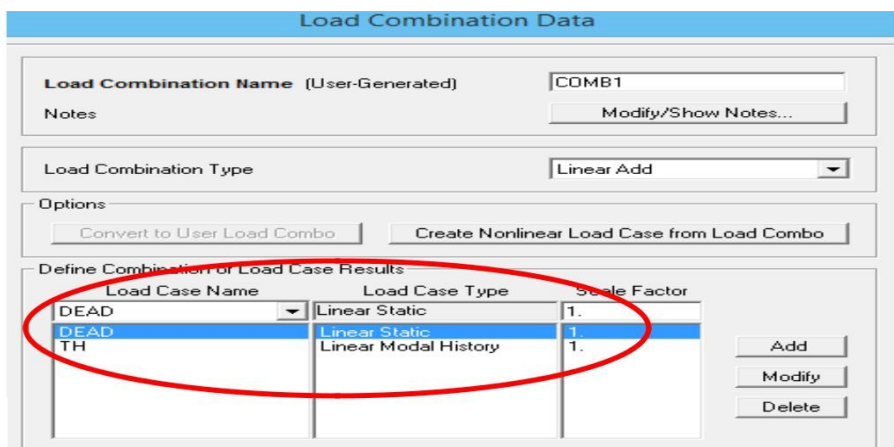


Figure 5.6: Steps in defining the loading

Finally the wall element was analysed after setting the analysis options and the displacement profile at each sensor locations were determined as presented in Figure 5.7.

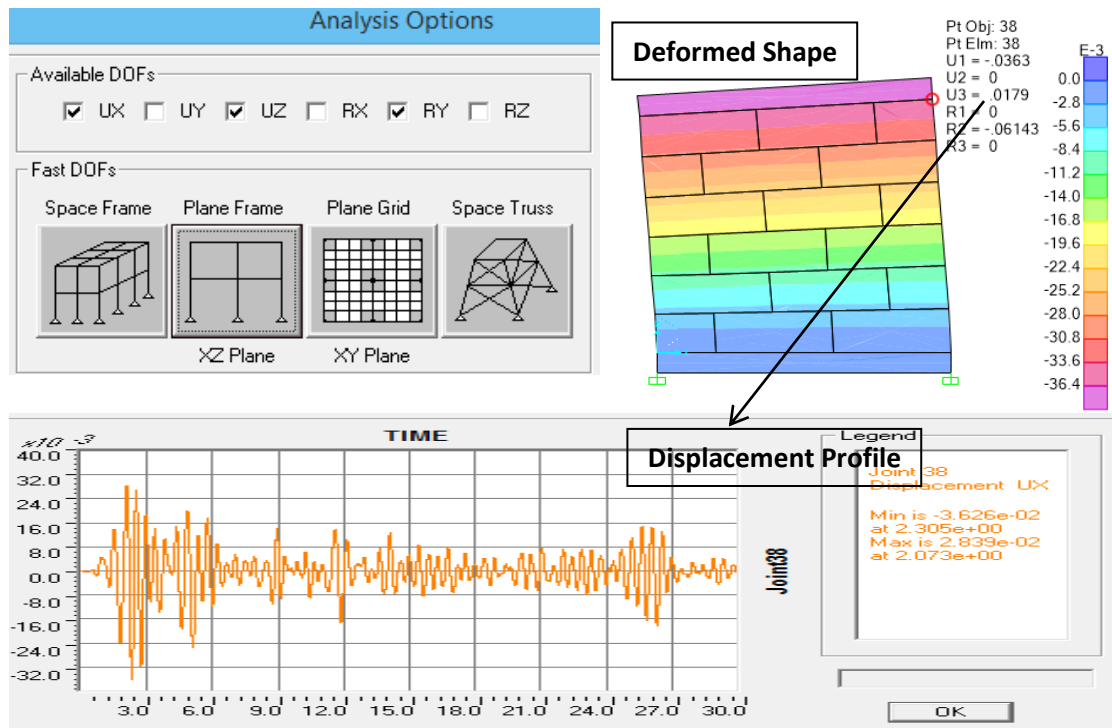


Figure 5.7: Analysis of SAP results

## 5.2 The Process of Numerical Modelling in ABAQUS

The following are the main steps of the dynamic analysis and the sequence of modelling the dynamic performance of earth walls using finite element software ABAQUS as illustrated in Figure 5.8.

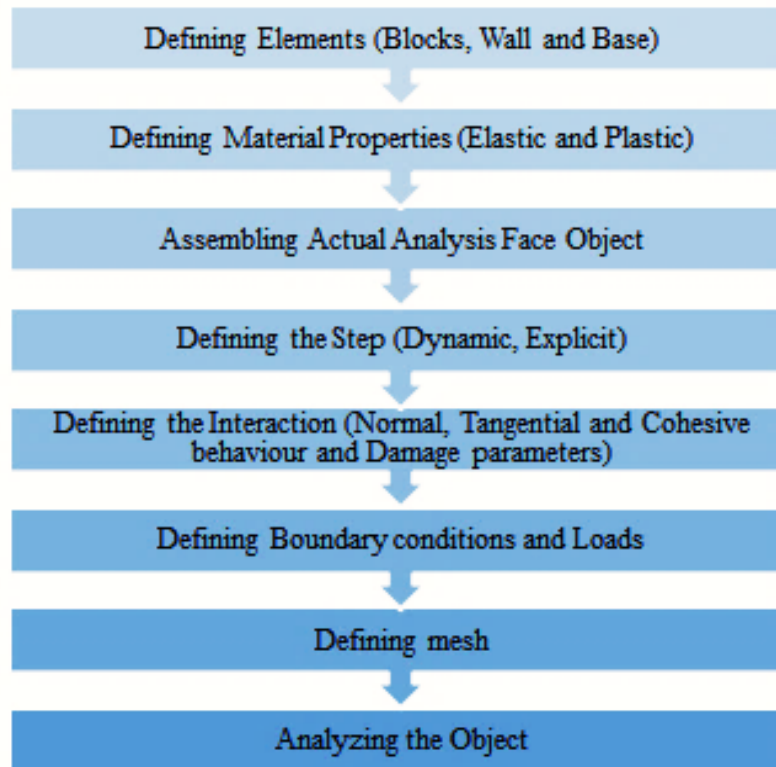


Figure 5.8: Steps of ABAQUS Modelling

### 5.2.1 Structural analysis using ABAQUS

The structural solving method used in the ABAQUS model was the “Explicit” method since it is a computationally efficient and can avoid convergence issues which can be highly occurred in “Implicit”.

Geometric non-linearity due to large displacements was included in all solving steps. The displacement output of the shake table at each test run was used as the input loading data of the numerical model. The objective of the simulation was to predict

the response and failure of specimens at each loading step. The following sections explain the features of the structural simulation.

### 5.2.2 Geometry

The geometry of the model was defined as 3D deformable solid. Earth masonry unit and mortar was modelled as one unit by expanding the block by  $\frac{1}{2}$  mortar thickness in one or both directions as illustrated in Figure 5-3. The element type of block and concrete layer was 8-node brick element with reduced integration (C3D8R). Steps in defining parts have been shown in Figure 5.9.

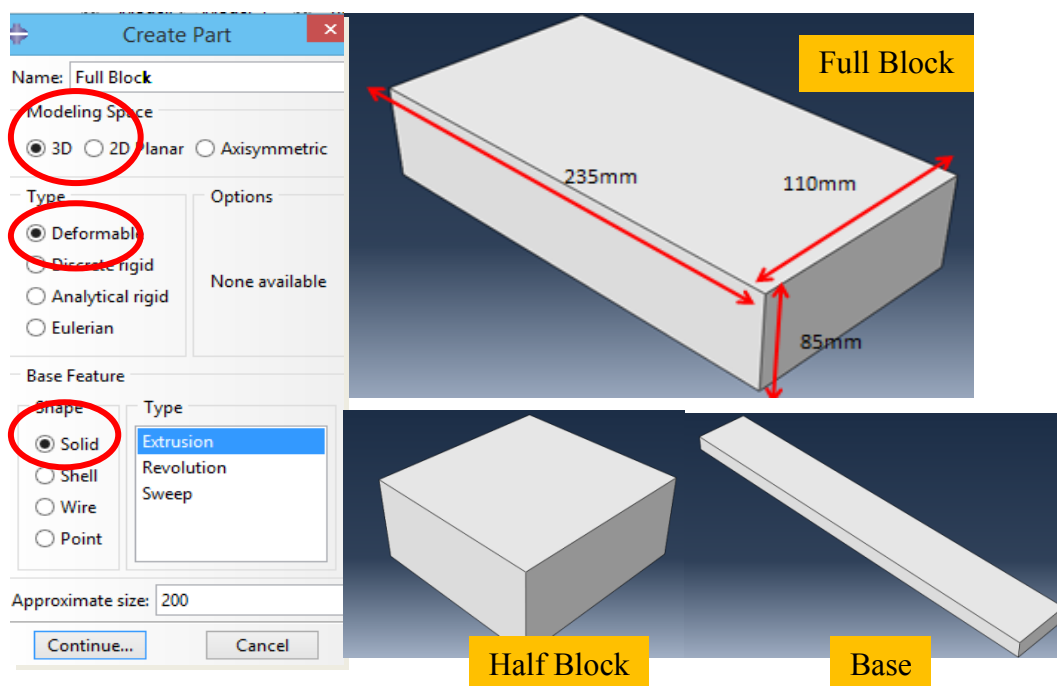
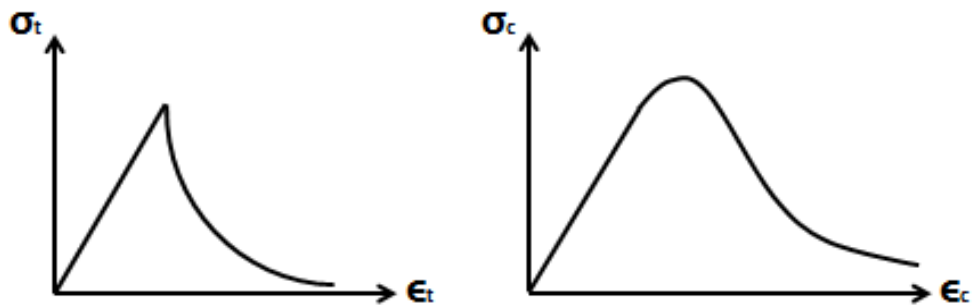


Figure 5.9: Defining the units

### 5.2.3 Material Properties

General, elastic and plastic properties were assigned to the block and mortar assemblage. In this mechanical modelling continuum approach (i.e. Concrete Damaged Plasticity model: CDP) was used for quasi-brittle materials subjected to cyclic loading. This approach uses the concepts of isotropic damaged elasticity with

isotropic tensile and compressive plasticity. Exponential and parabolic curves have been selected for tensile and compression behaviour as illustrated in Figure 5.10.



**Figure 5.10: Tensile and compression behaviour in CDP model**

#### **5.2.4 Assembling of the real object**

After defining the unit dimensions and material properties, all the units were arranged according to the real object under the ‘Assembly’ section of ABAQUS. Figure 5.11 shows the 3D view and elevation view of actual object.

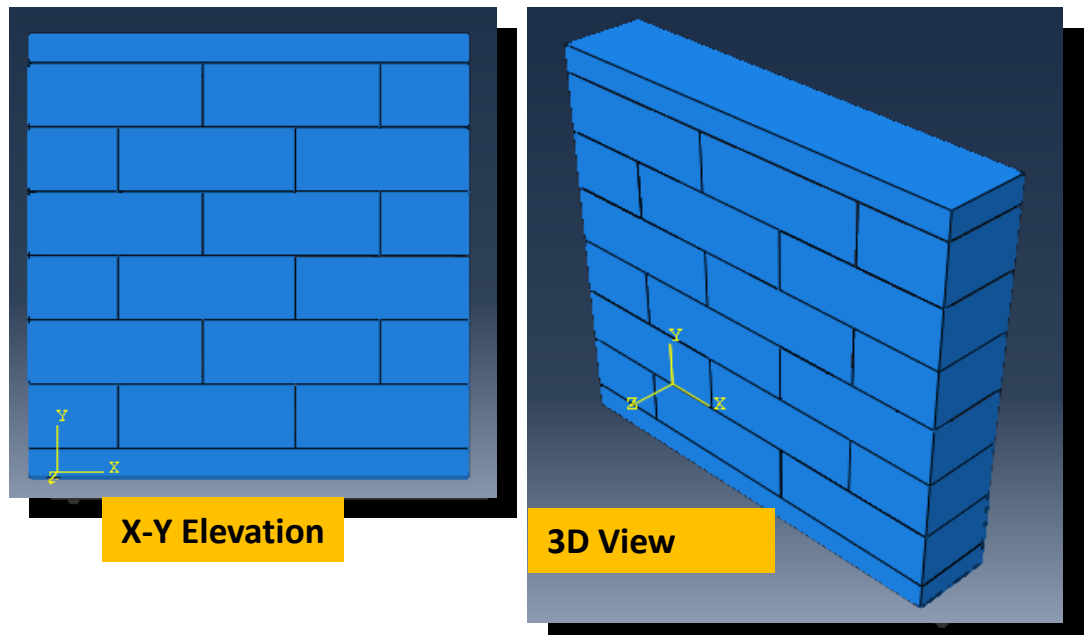


**Figure 5.11: Assembly of the real object in ABAQUS**



### 5.2.5 Interaction

Interaction between the contact surfaces was simulated through the friction and hard-contact type. In other words, friction interaction with 0.75 coefficient was defined for longitudinal behaviour and hard contact type interaction was defined for normal behaviour.

In addition to those contact properties cohesive behaviour and damage properties were assigned only for the horizontal contact surfaces since the cracks were initiated and propagated through the bed joints during the experiments.

As mentioned in Nezhad, et al, (2016) tensile and shear strength for mortar were considered as  $0.062\text{N/mm}^2$  and  $0.2\text{N/mm}^2$ . Further, the normal and shear stiffness were  $110\text{N/mm}^3$  and  $50\text{N/mm}^3$ .

### 5.2.6 Loading

Loading was applied as displacement with time. For an example, if the load is applied to the X-direction, during that time displacement in Y and Z directions were set to zero. The effect of self-weight was applied as a gravity load in the downward direction. Figure 5.12 demonstrates the view of the wall element after the application of seismic load and gravity load.

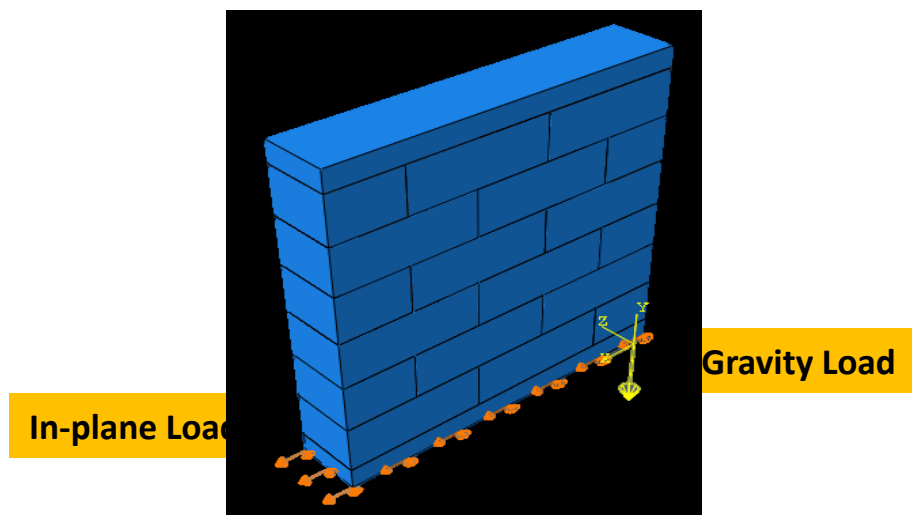


Figure 5.12: Loading in ABAQUS

## 5.2.7 Meshing

Meshing size of each unit should be reduced in order to predict the actual behaviour of the model as in Figure 5.13. But for the lesser computational time increased mesh size was selected.

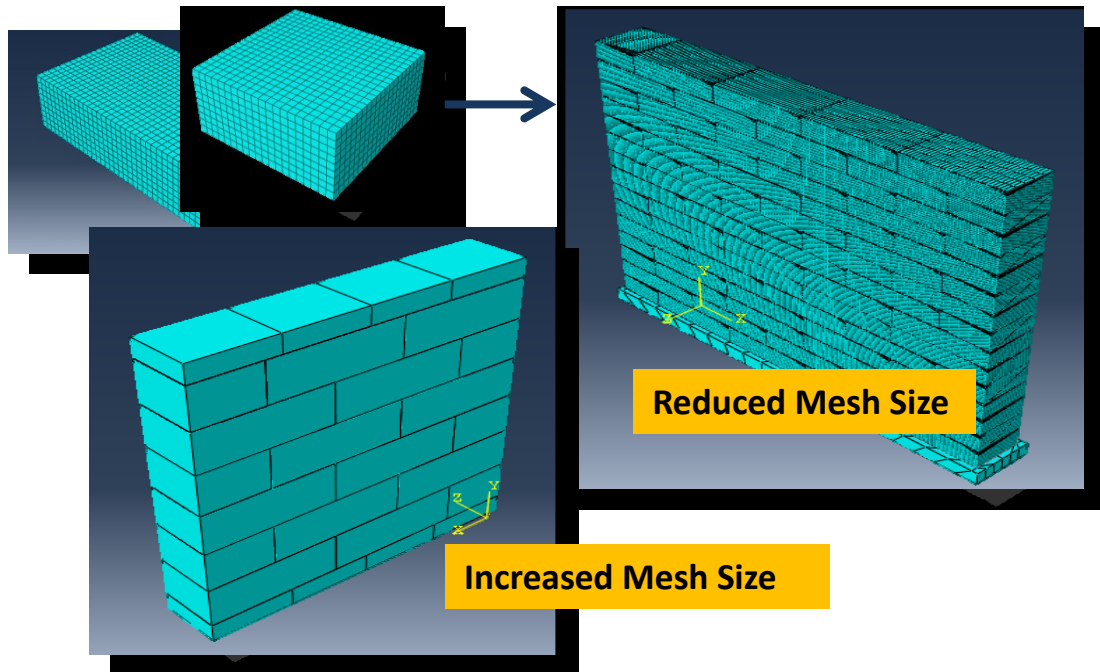


Figure 5.13: Meshing the object in ABAQUS

Finally the wall element was analysed after setting the analysis options and the displacement profile at each sensor location was determined as presented in Figure 5.14.

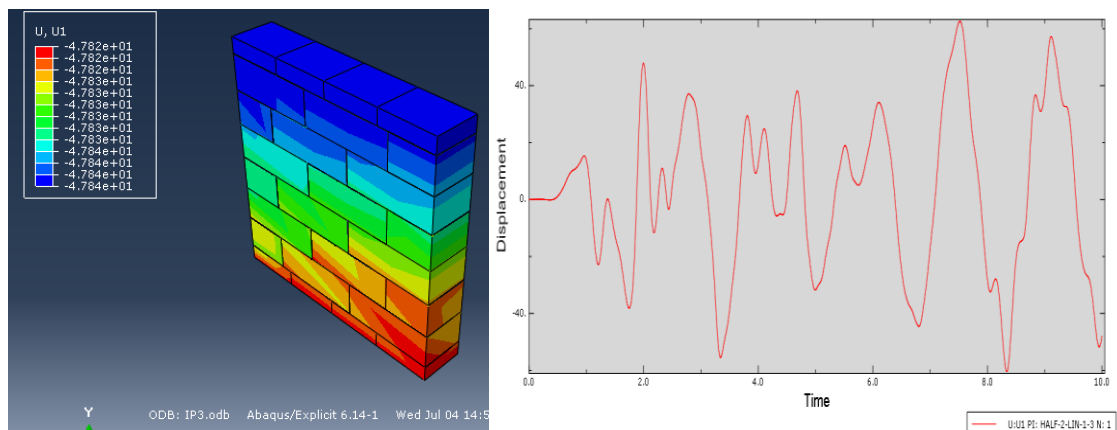


Figure 5.14: Analysis of ABAQUS results

### 5.3 Comparison of SAP and ABAQUS numerical results

Numerical displacement results in the middle and the top of the walls under the in-plane loading marginally coincide with the experimental results and for the out-of-plane loading, numerical results at the middle of the wall only marginally coincide with the experimental results. The comparison graphs for the in-plane can be plotted as Figure 5.15.

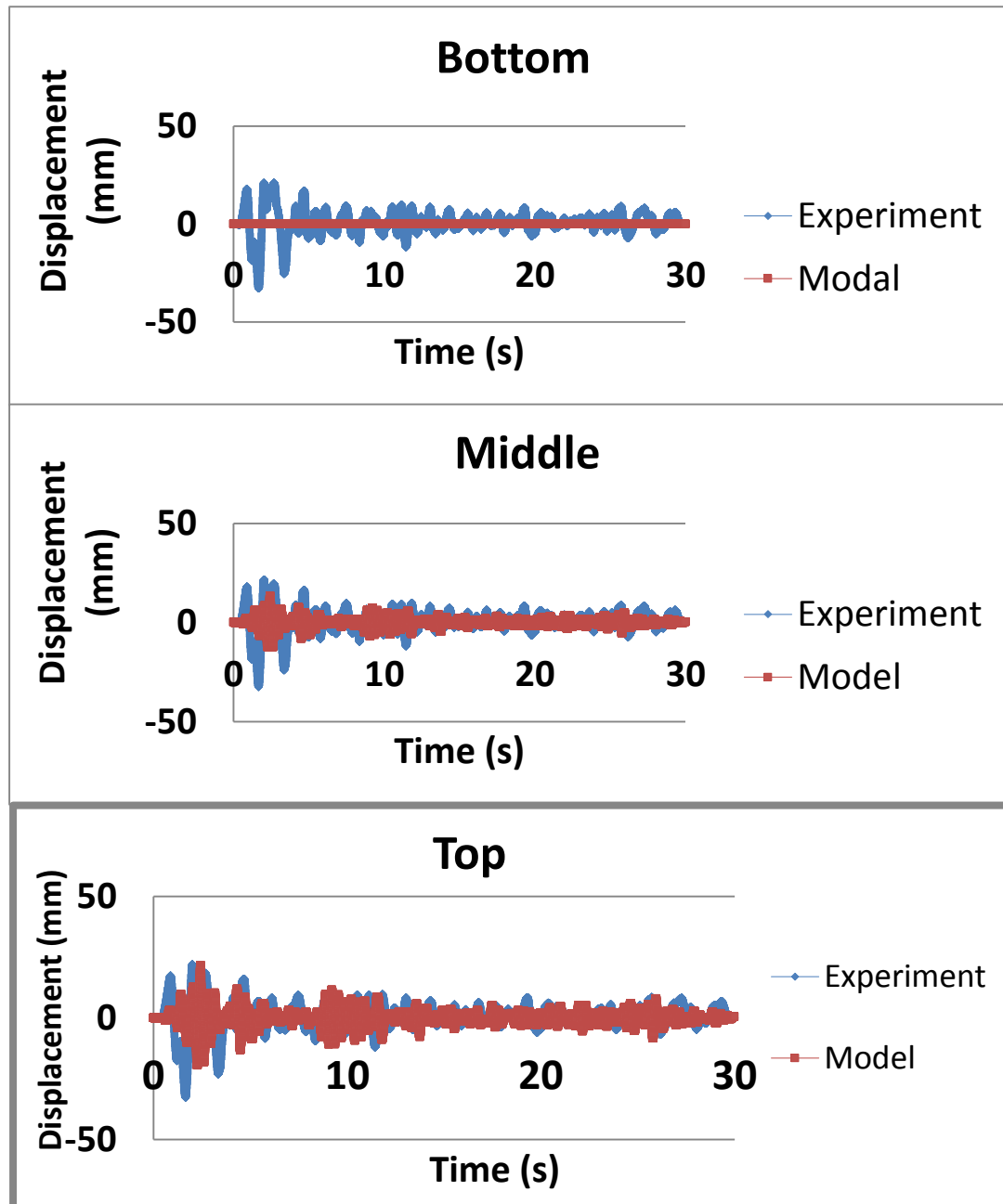


Figure 5.15: SAP numerical results

Numerical displacement results at the bottom, middle and the top of the walls under the in-plane and out-of-plane loading considerably coincide with the experimental results. The comparison graphs for out-of-plane can be plotted as Figure 5.16.

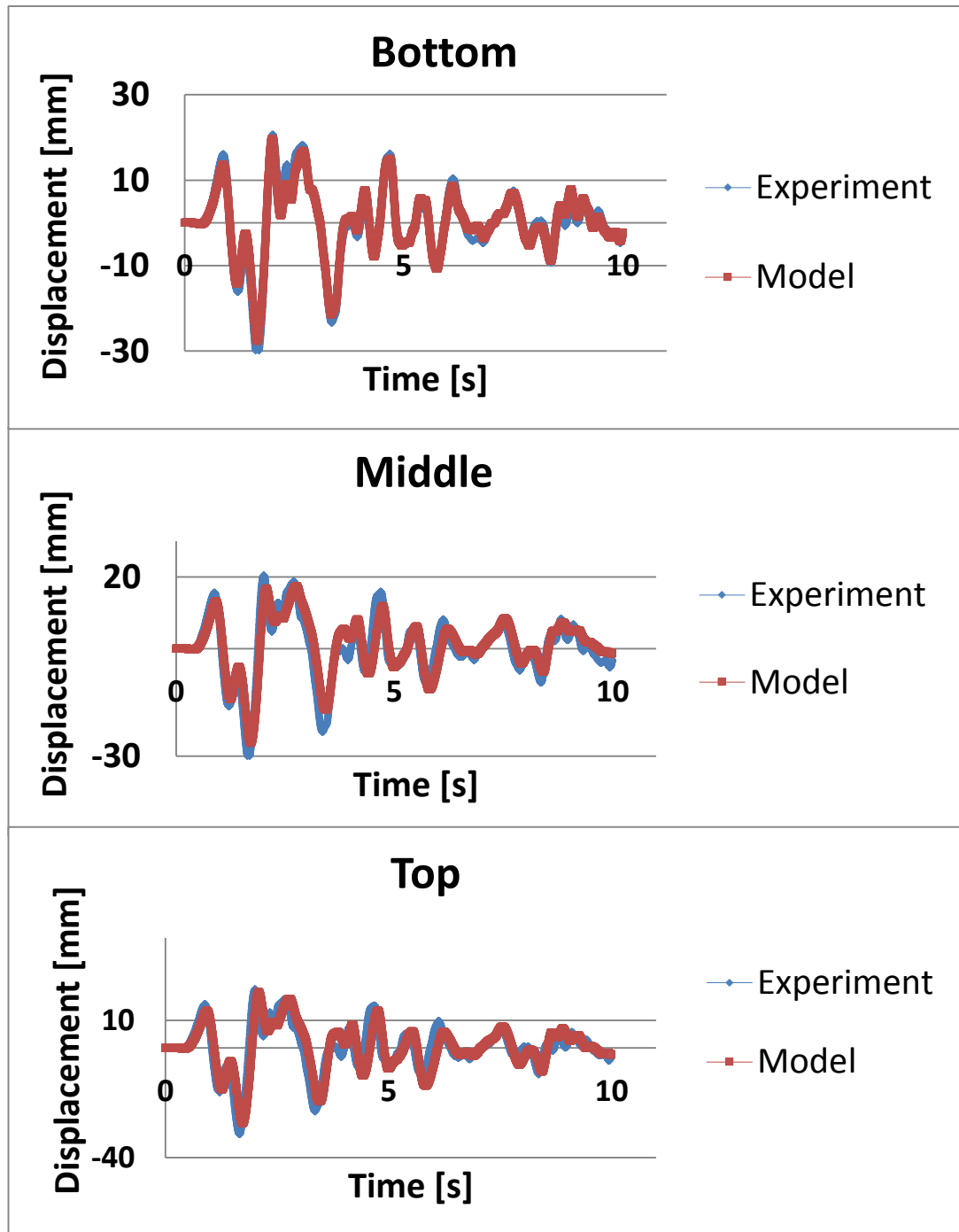


Figure 5.16: ABAQUS numerical results

**Table 5.1: Comparison of two computational models**

Item considered	SAP	ABAQUS
Geometry Modelling	Micro-macro model	Micro-macro model
Material Properties	Elastic and Takeda Hysteresis with Drucker Prager model	Elastic and Concrete Damage Plasticity model
Assembling the actual element	Following Grid Pattern	Movement of elements
Defining the analysis type	Either modal or time history load case	Explicit solver
Interaction	Provide edge area constraints	Surface contact through tangential, normal, cohesive behaviour and damage
Defining the loads	Defining time history function	Defining displacement function and apply on the surface
Boundary Condition	Fixed at the bottom (Unless, huge distortions of the model)	Can apply displacement and acceleration constraints separately
Meshing the objects	Coarse mesh	Coarse mesh
Duration of analysis	Less than one minute	About fifteen minutes
Displacements	Marginal convergence	Greater convergence

Table 5.1 illustrates the comparison of experimental results with the results of numerical models of SAP and ABAQUS.

In SAP, actual object was assembled according to the grid pattern using micro-macro element approach. Masonry was assumed as anisotropic and the Takeda hysteresis model was used. The bottom of the object should be restrained, and edge area constraint must be applied to avoid model distortions.

In ABAQUS, actual object was assembled using 3D stress elements following micro-macro element approach. Masonry was assumed as isotropic and the concrete damage plasticity model was used. Surface interaction was applied through tangential, normal and cohesive behaviour and damage parameters. The dynamic explicit solver was used to analyse the object under displacement vs time function.

There are limitations in the SAP model to apply, true boundary and contact properties. Therefore, displacement values of the wall do not coincide with the experimental results. In the ABAQUS model, above limitations can be overcome and hence the results are considerably within the experimental values. But more sectional and material properties inherent to the actual structure should input in order to get accurate results and further solving time is much higher compared to SAP.

Hence, ABAQUS modelling of was selected to numerically model the behaviour of earth structures for other loading categories as well.

Two different comparisons have been undertaken to validate the accuracy of the finite element model using the general finite element package ABAQUS.

- i) Verification for displacement vs. time under moderate to severe earthquakes.
- ii) Verification of failure stresses under moderate to severe earthquakes and at the sine wave that caused failure.

Similar to the Chapter 5, CSEB blocks, CSRE wall specimen and concrete layers were modelled using the solid element C3D8R. Blocks and wall panel were expanded by half the mortar dimension in both directions and applied the surface to surface contact properties such as tangential, normal, cohesive and damage interaction. Tangential behaviour was with friction coefficient of 0.75 and normal behaviour was with “Hard” contact type. As mentioned in Nezhad et al. (2016), tensile and shear strength for mortar was considered as 0.062N/mm<sup>2</sup> and 0.2N/mm<sup>2</sup> and normal and shear stiffness were considered to be 110N/mm<sup>3</sup> and 50N/mm<sup>3</sup>. Concrete damaged plasticity model was used for the materials as it

predicts the behaviour of quasi-brittle materials under cyclic loading. Explicit solver in ABAQUS was chosen as it is a computationally efficient and has low convergence problems over implicit method. Loading was applied as a displacement with time. Meshing size of each unit should be reduced in order to predict the actual behaviour of the model. But for the lesser computational time increased mesh size was selected. CSEB out-of-plane wall model representation and its displacement output at a specific step time are presented in Figure 5.17.

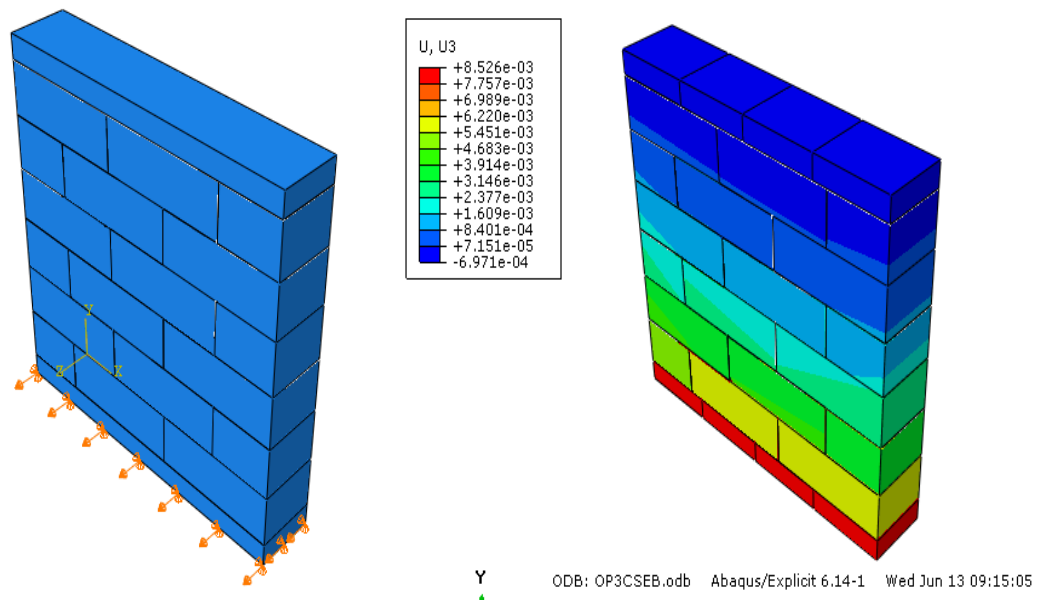


**Figure 5.17: CSEB wall numerical model**

Agreement between the numerical and experimental results of CSEB and CSRE wall panels is presented in Table 5.2.

Table 5.2: Comparison of Numerical Modelling Results with Experimental

Displacement vs. Time	
CSEB Wall Panel	CSRE Wall Panel
<p style="text-align: center;"><b>1.72EI In-Plane</b></p> <p style="text-align: center;"><b>1.72EI Out-of-Plane</b></p>	<p style="text-align: center;"><b>1.72EI In Plane</b></p> <p style="text-align: center;"><b>1.72EI Out-of-Plane</b></p>
<p><b>Figure 5.18: CSEB Displacement vs. Time</b></p> <p>Numerical displacement results at the bottom, middle and the top of the walls from moderate to severe earthquakes under the in-plane and out-of-plane loading considerably coincide with the experimental results. The comparison graphs for in and out-of-plane loading under the severe earthquake can be plotted as Figure 5.18.</p>	<p><b>Figure 5.19: CSRE Displacement vs. Time</b></p> <p>Numerical displacement results at the bottom, middle and the top of the walls from moderate to severe earthquakes under the in-plane and out-of-plane loading considerably coincide with the experimental results. The comparison graphs for in and out-of-plane loading under the severe earthquake can be plotted as Figure 5.19.</p>



## Failure Loading Step and Type

CSEB Wall Panel	CSRE Wall Panel
<p style="text-align: center;"><b>Figure 5.20: Failure Stresses of CSEB walls</b></p> <p>CSEB in-plane walls did not fail and out-of-plane walls failed under the rocking mode at the base during the 6Hz wave. In other words, during the 6Hz wave in the out-of-plane walls, tensile stresses of lowest bed joint exceeds the tensile strength. When we model the 6Hz wave scenario and check the stresses in S23 direction, it can be highlighted that the maximum stresses are at the base and exceeds the tensile strength value of 0.062N/mm<sup>2</sup> [Nezhad et al.(2016)] as plotted in Figure 5.20.</p>	<p style="text-align: center;"><b>Figure 5.21: Failure Stresses of CSRE walls</b></p> <p>RE in-plane and out-of-plane walls failed under the shear and rocking mode at the base during the 6Hz wave. In other words, during the 6Hz wave in the out-of-plane walls, tensile stresses of lowest bed joint exceeds the tensile strength. When we model the 6Hz wave scenario and check the stresses in S23 direction, it can be highlighted that the maximum stresses are at the base and exceeds the tensile strength value of 0.062N/mm<sup>2</sup> [Nezhad et al.(2016)] as plotted in Figure 5.21.</p> <p>Similarly, during the 6Hz wave in the in-plane walls, shear stresses of lowest bed joint was exceeded the shear strength. When we model the 6Hz wave scenario and check the stresses in S12 direction, it can be highlighted that the maximum stresses are at the base and close to the 0.2N/mm<sup>2</sup> [Nezhad et al.(2016)] as plotted in Figure 5.21.</p>

## **6. CONCLUSION AND FUTURE WORK**

Shake table tests were carried out for full scale CSEB and CSRE wall panels with locally available soil to investigate their behavior with respect to loading direction, magnitude and then developed a numerical model validated with experimental results. The dimensions of wall panels were selected based on previous research and limited due to the shake table capacities. Two walls of each earth masonry type were cast and loaded them in-plane and out-of-plane.

The test panels were loaded under the two categories. The first category was an actual earthquake (North-South component of 1940 El-Centro earthquake) with three different scales and the second was a sine wave with four different frequencies and amplitudes.

The behavior of walls was studied in terms of displacement and acceleration response, base shear, failure magnitude and type.

According to the experimental results from moderate to severe earthquakes, both CSEB and CSRE wall panels performed well without any visible cracks. In CSEB wall panels, maximum acceleration and displacement at the crest of the wall and base shear is 8.2%, 1.2% and 7.6% greater in out-of-plane loads than the in-plane walls under severe earthquake. But in CSRE wall panels those above considered values remain same for both in and out-of-plane walls.

In order to investigate the progressive damage behavior of earth walls, they subjected to sine waves with increasing amplitudes and frequencies. In CSEB walls, there were no visible cracks both in and out-of-plane walls until the 4Hz sine wave. But when the frequency become 6Hz, base crack was initiated and spread throughout the wall width in the out-of-plane wall and no visible cracks in the in - plane wall. In CSRE walls, there were no visible cracks both in and out-of-plane walls until the 4Hz sine wave. But when the frequency become 6Hz, base crack was developed through the wall width with rocking mode in the out-of-plane wall and base crack was developed

with some translation to the loading direction in the in-plane wall. Hence, strengthening should be carried out at the base of the walls.

General finite element package ABAQUS was used to numerically model the seismic response of earth masonry walls and two different comparisons (displacement, failure type and magnitude) have been undertaken to validate the accuracy of finite element model.

Numerical results showed a good agreement with the experimental results in terms of displacement and failure mechanism and the developed method can be used to numerically model the real scale structural elements and study their seismic performance.

In this study, the dimensions of the wall panels were selected as per the payload capacity of the shaking table. In order to consider the scale effect of the wall panels, it is recommended to go for a larger capacity shake table in future.

## **6.1 Future Work**

The findings were based upon the study of one replicate. Therefore, better to confirm those results with many models in each configuration and varying the parameters like;

- Building height
- Width of wall thickness
- Scale of the structure
- Opening sizes
- Pre-compression load
- Block pattern
- Number of floors of the model
- Interior structural arrangement of the model
- Modelling application

According to the observed failure patterns in the wall panels, the possibility of enhancing their seismic capacity can be observed in future studies by adopting some earthquake resistant features such as reinforced concrete bands, PP-bands, GFRP strips, wire mesh, etc in weak regions of the wall panels.

The accuracy of the results is the direct outcome of element type, material properties, boundary conditions, interaction properties, loading condition and mesh size and control. Therefore, with the developed model, a sensitivity analysis can be carried out for the above-mentioned parameters.

### **Acknowledgements**

Funding provided by University of Moratuwa and non-academic staff of Department of Civil Engineering, University of Moratuwa.

### **References**

- R. Bahar, M. Benazzoung, and S. Kenai, "Performance of compacted cement stabilized soil", *Cement and concrete composites*, vol.26, pp. 811-820, 2006.
- M. Betti, L. Galano, and A. Vignoli, "Comparative analysis on the seismic behaviour of unreinforced masonry buildings with flexible diaphragms", *Eng. Str.*, vol.61, pp.195-208, 2014.
- M. Blondet, J. Vargas, J. Velásquez, and N. Tarque, "Experimental study of synthetic mesh reinforcement of historical adobe buildings", in *Proceedings of Structural Analysis of Historical Constructions, New Delhi, India*, 2006. pp.1-8.
- A. Bulkhi, "25 Worst Earthquakes in History", 2016.[Online].Available : <https://list25.com/25-worst-earthquakes-in-history/>. [Accessed: 10-Jul-2018].
- E. Çaktı, Ö. Saygılı, J.V. Lemos, and C.S. Oliveira, "Discrete element modeling of a scaled masonry structure and its validation", *Eng. Str.*, vol. 126, pp.224-236, 2016.
- V. P. P. Cole, E.F. Gad, C. Clifton, N.T.K. Lam, C. Davies, and S. Hicks, "Out-of-plane performance of a brick veneer steel-framed house subjected to seismic loads", *Constr. Build. Mater.*, vol.28, pp.779-790, 2012.
- K.M. Dolatshahi, and A.J. Aref, "Three Dimensional Modeling of Masonry Structures and Interaction of In-Plane and Out-of-Plane Deformation of Masonry Walls", *Engineering Mechanics Institute Conference*, 2011.
- "El Centro Earthquake-Vibrationdata", [Online].Available : <http://www.vibrationdata.com/elcentro.htm>. [Accessed: 04-Aug-2017].

- K.A. Heathcote, "Durability of earth wall buildings", *Constr. Build. Mater.* vol. 9(3), pp 185-189, 1995.
- R. Illampas, D.C. Charmpis, and I. Ioannou, "Laboratory testing and finite element simulation of the structural response of an adobe masonry building under horizontal loading", *Eng. Str.*, vol. 80, pp. 362-376, 2014.
- C. Jayasinghe, and N. Kamaladasa, "Compressive strength characteristics of cement stabilized rammed earth walls", *Constr. Build. Mater.*, vol. 21, pp.1971-1976, 2007.
- C. Jaysinghe, and R.S. Mallawaarachchi, "Flexural strength of compressed stabilized earth masonry materials", *Materials and Design*, Elsevier, vol.30, pp. 3859-3868, 2009.
- L. Kai, W. Ming, and W. Yaan, "Seismic retrofitting of rural rammed earth buildings using externally bonded fibers", *Constr. Build. Mater.*, vol.100, pp.91-101, 2015.
- L. Keshav, V. G. Srisanthi, and G. Balamurugan, "Shaking Table Study of Two Reduced-Scale Single-Storey HCSE Block Masonry Building Models", *Civil Engineering*, DOI 10.1007/S13369-013-0893-6, 2013.
- M. Lorenzo, D. Anastasios, and M. Urs, "In-plane behaviour of rammed earth under cyclic loading: Experimental testing and finite element modeling", *Eng. Str.*, vol.125, pp.144-152, 2016.
- M., Lorenzo, M. Urs, and P. Stanislav, "Rammed earth walls strengthened with polyester fabric strips: Experimental analysis under in-plane cyclic loading", *Constr. Build. Mater.*, vol.149, pp.29-36, 2017.
- P.B. Lourenço, L. Avila, G. Vasconcelos, J. P. Alves, N. Mendes, and A.C. Costa, "Experimental investigation on the seismic performance of masonry buildings using shaking table testing", *Bull Earthquake Eng.*, vol.11, pp.1157-1190, 2013.
- R. Ma, L. Jiang, M. He, C. Fang, and F. Liang, "Experimental investigations on masonry structures using external pre-stressing techniques for improving seismic performance", *Eng. Str.*, vol.42, pp.297-307, 2012.
- E.A.Mehmet, and E. M, Y.Ahmet, "Structural behaviour of rammed earth walls under lateral cyclic loading: A comparative experimental study", *Constr. Build. Mater.*, vol. 133, pp.433-442, 2017.
- Meillyta, "Finite Element Modelling of Unreinforced Masonry (URM) Wall with Openings": *Studies in Australia, The Proceedings of 2nd Annual International Conference Syiah Kuala University 2012 & 8th IMT-GT Uninet Biosciences Conference Banda Aceh*, 2012. pp.22-24.
- R. Nabouch, Q.B. Bui, O. Ple, P. Perrotin, C. Poinard, T. Goldin, and J.P. Plassiard, "Seismic assessment of rammed earth walls using pushover tests", *Cons. Build. Mater.*, vol.145, pp.1185-1192, 2016.

- S. Nayak, and S.C. Dutta, "Failure of masonry structures in earthquake: A few simple cost effective techniques as possible solutions", *Eng. Str.*, vol.106, pp.53-67,2016.
- R.S. Nezhad, M.Z. Kabir, and M. Banazadeh, "Shaking table test of fibre reinforced masonry walls under out-of-plane Loading", *Constr.Build.Mater.*, vol.120, pp. 89-103, 2016.
- X. Palios, M. N. Fardis, E. Strepelias, and S.N. Bousias, "Un-bonded brickwork for the protection of infills from seismic damage", *Eng. Str.*, vol.131,pp.614-624, 2017.
- S. Priyantha, "Seismic hazard assessment for Colombo city with local site effects", *Research Project for Master of Engineering, Department of Civil Engineering, University of Moratuwa, Sri Lanka*, 2016.
- V. Ratnam, "Development of Earthquake resistant designs, methodologies and construction technologies for masonry buildings in Sri Lanka". *Research Project for Master of Engineering in Structural Engineering Design, Department of Civil Engineering, University of Moratuwa, Sri Lanka*, 2014.
- B.V. Reddy, and J.S. Jagadish,"Properties of soil-cement block masonry", *Masonry International, British Masonry Society*, vol. 3(2), pp 80-84,1989.
- M. U. Saleem, M. Numada, M. N. Amin, and K. Meguro, "Seismic response of PP-band and FRP retrofitted house models under shake table testing", *Constr.Build.Mater.*, vol. 111,pp. 298-316, 2016.
- A. Sánchez, G. Solar, P.E. Martín, and N.G. Maldonado, "Surface Interaction Model for Great thickness Masonry", *Frontiers in Built Environment*, DOI:10.3389/fbuil.2017.00025.
- D.G. Sapir, and F. Vos, "Human Casualties in Earthquakes", *An Epidemiological Perspective on Patterns and Trends*, pp. 322, ISBN: 978-90-481-9454-4, 2011.
- B. Silva, M.D. Benetta, F. Porto, and C. Modena, "Experimental assessment of in-plane behavior of three-leaf stone masonry walls", *Constr.Build.Mater.*, vol.53,pp.149-161,2014.
- S.S. Sivaraja, T.S. Thandavamoorthy, S. Vijayakumar, S. Mosesaranganathana, P.T. Rathnasheela, and A.K. Dasarathy, "GFRP Strengthening and Applications of Unreinforced Masonry wall (UMW)", *Procedia Engineering*, vol.54, pp.428-439, 2013.
- V.G. Srisanthi, L. Keshav, P.P. Kumar, and T. Jayakumar, "Finite element and experimental analysis of 3D masonry compressed stabilized earth block and brick building models against earthquake forces", *Civil Engineering*, 58/3(2014)255-265.

N. Tarque, G. Camata, E. Spacone, M. Blondet, and H. Varum, “The use of continuum models for analysing adobe structures”, *Constr.Build.Mater.*, vol.28,pp.779-790,2012.

P. Vidal, P.Cole , E. F. Gad , C.Clifton , N.T.K. Lam , C.Davies, and S.Hicks, “Out-of-plane performance of a brick veneer steel-framed house subjected to seismic loads”,2012.

W. Yaan, W. Ming, L. Kai, P. Wen, and Y. Xiaodong, “Shaking table tests on seismic retrofitting of rammed earth structures”, *Bull Earthquake Eng.* (2016)DOI:10.1007/s10518-016-9996-2.